Am J Physiol Renal Physiol 315: F1565–F1582, 2018.
First published August 8, 2018; doi:10.1152/ajprenal.00510.2017.

RESEARCH ARTICLE

Section-specific expression of acid-base and ammonia transporters in the kidney tubules of the goldfish *Carassius auratus* and their responses to feeding

Sandra Fehsenfeld and Chris M. Wood

University of British Columbia, Department of Zoology, Vancouver, Canada

Submitted 16 October 2017; accepted in final form 6 August 2018

Fehsenfeld S, Wood CM. Section-specific expression of acid-base and ammonia transporters in the kidney tubules of the goldfish *Carassius auratus* and their responses to feeding. *Am J Physiol Renal Physiol* 315: F1565–F1582, 2018. First published August 8, 2018; doi:10.1152/ajprenal.00510.2017.—In teleost fishes, renal contributions to acid-base and ammonia regulation are often neglected compared with the gills. In goldfish, increased renal acid excretion in response to feeding was indicated by increased urine ammonia and inorganic phosphate concentrations and decreased urine pH. By microdissecting the kidney tubules and performing quantitative real-time PCR and/or immunohistochemistry, we profiled the section-specific expression of glutamate dehydrogenase (GDH), glutamine synthetase (GS), Na^+/H^+-exchanger 3 (NHE3), carbonic anhydrase II (CAIIa), V-H^+-ATPase subunit 1b, Cl^-/HCO_3^--exchanger 1 (AE1), Na^+/HCO_3^--cotransporter 1 (NBC1), Na^+/K^+-ATPase subunit 1α, and Rhesus-proteins Rhbg, Rhcg1a, and Rhcg1b. Here, we show for the first time that *1*) the proximal tubule appears to be the major site for ammoniagenesis, *2*) epithelial transporters are differentially expressed along the renal tubule, and *3*) a potential feeding-related "acidic tide" results in the differential regulation of epithelial transporters, resembling the mammalian renal response to a metabolic acidosis. Specifically, GDH and NHE3 mRNAs were upregulated and GS downregulated in the proximal tubule upon feeding, suggesting this section as a major site for ammoniagenesis and acid secretion. The distal tubule may play a major role in renal ammonia secretion, with feeding-induced upregulation of mRNA and protein for apical NHE3, cytoplasmic CAIIa, universal Rhcg1a and apical Rhcg1b, and downregulation of basolateral Rhbg and AE1. Changes in mRNA expression of the Wolffian ducts and bladder suggest supporting roles in fine-tuning urine composition. The present study verifies an important renal contribution to acid-base balance and emphasizes that studies looking at the whole kidney may overlook key section-specific responses.

acidosis; ammoniagenesis; freshwater teleost; protein and mRNA expression; renal epithelium

INTRODUCTION

The maintenance of acid-base homeostasis is one of the most important physiological processes from cell to organism, as it ensures proper enzyme and protein function. On a long-term basis, the major organ counteracting any acid-base disturbance in mammals is the kidney, which adjusts net renal acid (both titratable acid and NH_4^+ fluxes) and base (HCO_3^-) excretion as needed (25). An important process in this context is renal ammoniagenesis, generating equimolar amounts of HCO_3^- and NH_4^+ (74) and, hence, directly regulating the concentration of these acid-base components in both the urine and extracellular fluid. In contrast, the teleost kidney generally seems to make only a small contribution (~5–30%) (54) to *1*) general net acid excretion and *2*) to compensating many common acid-base disturbances (i.e., hypercapnia- (23, 53) or hyperoxia-induced respiratory acidosis (77) and feeding-induced alkaline tide (5) in gastric fishes, such as the freshwater trout *Oncorhynchus mykiss*). The gills are normally considered far more important for both acid-base regulation (54) and ammonia excretion (85). However, in response to a metabolic acidosis caused by exposure to low environmental pH, the renal contribution to net acid excretion increases greatly in goldfish *Carassius auratus* (36, 39), freshwater trout (46, 83), and common carp *Cyprinus carpio* (86), because under this scenario, the gills are taking up acid on a net basis, and the kidney becomes the only route for acid excretion. The kidney also plays an important role in compensating metabolic acidosis caused by direct systemic injection of acid loads, in both the channel catfish *Ictalurus punctatus* (13) and rainbow trout *Oncorhynchus mykiss* (82).

In addition to challenges for their acid-base homeostasis, freshwater teleosts face the constant threat of losing ions to their dilute environment, while at the same time, generating high flow rates of urine to compensate for osmotic water influx. Hence, the reabsorption of ions from the urine is critically important in these animals (20, 55, and references therein; 77). Interestingly, the absorption and secretion of ions were affected by disturbances of acid-base homeostasis, such as responses to hyperoxia in freshwater trout (77) or low environmental pH in common carp (86) and goldfish (39), or generally, when urine flow was affected due to an acid-base challenge (36, 45). Inevitably, renal ion regulation depends on epithelial transporters that also directly or indirectly regulate fluxes of acid-base equivalents. Indeed, many of the epithelial transporters found in the teleost gill and known to be involved in branchial acid-base regulation are also associated with the mammalian (74) and teleost kidney (55). Additionally, Rhesus glycoproteins that act as ammonia channels (43, 84) and play an important role in branchial ammonia excretion in fishes (85) can also be found in teleost (86) and mammalian (74) kidneys, potentially linking acid-base with ammonia regulation. Two recent studies in goldfish (39) and common carp (86) showed that the Rhesus glycoprotein isoforms Rhbg, Rhcg1a (also named Rhcg1 or Rhcga), and Rhcg1b (also named Rhcg2 or

Address for reprint requests and other correspondence: S. Fehsenfeld, Univ. of British Columbia, Dept. of Zoology, 6270 University Blvd., Vancouver, BC Canada V6T 1Z4 (e-mail: Fehsenfeld@zoology.ubc.ca).

Rhcgb), indeed, undergo differential changes in renal mRNA expression in response to a metabolic acidosis. Therefore, in specific situations, renal acid-base and ammonia regulation appear to be important for overall systemic acid-base and ammonia homeostasis in teleost fishes.

Studies to date have looked at gene expression only in the teleost kidney as a whole, even though much of its complex microstructure resembles that of the mammalian kidney (21, and references therein; 74). Indeed, the specific diversification into different tubule sections has been characterized for the goldfish kidney by Sakai (62). Though present knowledge is sparse, some parallels seem to exist between teleosts and mammals. In mammals, renal ammoniagenesis is mainly associated with glutamine metabolism in the proximal tubules. Two of the key enzymes involved, phosphate-dependent glutaminase (PDG) and glutamate dehydrogenase (GDH), as well as other ammoniagenic enzymes, including alanine aminotransferase, are also present in the teleost kidney, and increase in activity in response to a metabolic acidosis in freshwater rainbow trout (83) and goldfish (39). The major driver for the secretion of ammonia from ammoniagenesis in the mammalian proximal tubule seems to be the apical Na^+/H^+-exchanger (NHE3) (53). In freshwater rainbow trout, NHE3 is highly expressed immunochemically in the apical membrane of proximal tubules in colocalization with H^+-ATPase (HAT), and its whole kidney mRNA expression increases in response to a hypercapnia-induced respiratory acidosis (30). Interestingly, Rhesus glycoproteins and, specifically, the apical Rhcg were only weakly expressed in this section in the common carp (86). However, strong Rhcg/Rhcg1a expression has been identified by immunohistochemistry (IHC) in the apical distal tubule (DT), and it seemed to increase in response to a metabolic acidosis in both mammals (64) and teleosts (86). Interestingly, by IHC, the mangrove rivulus *Kryptolebias marmoratus* (17) showed a coexpression of Rhcg1a with apical NHE3 protein in the DT and, hence, the potential promotion of ammonia secretion also in this section. Because of the presence of $Na^+/K^+/2Cl^-$-cotransporter (NKCC), the teleost DT has been considered as functionally analogous to the thick ascending limb (TAL) of the mammalian kidney (21, 33). Teleosts themselves, however, lack a loop of Henle and consequently, a directly homologous structure to the TAL (21, and references therein; 62). The complex function of the mammalian collecting duct (CD) involves multiple processes contributing to acid-base and ammonia homeostasis, including basolateral ammonia transport via Rhbg, Rhcg, and Na^+/K^+-ATPase (NKA), cytosolic proton production via carbonic anhydrase CAII, apical ammonia secretion via Rhcg, apical proton secretion involving HAT and H^+/K^+-ATPase, as well as basolateral bicarbonate transport via Cl^-/HCO_3^--exchanger (74). Very little is known about the function of the CD in teleosts, but some of these epithelial transporters have been identified there by IHC, including Rhcg1a in zebrafish *Danio rerio* (50) and NKA in the goldfish (15).

To date, the impact of the essential process of feeding on the physiology of acid-base and ammonia transport in teleost fishes has received little study at the molecular level. Feeding has been shown to generate a systemic base load ("alkaline tide") in teleosts with acid-secreting stomachs such as trout (9, 18) and a systemic acid load ("acidic tide") in agastric fishes with base-secreting intestines such as the freshwater killifish *Fundulus heteroclitus* (81), as well as an ammonia load in both (9, 18, 81, 87). The goldfish *C. auratus* is agastric, so an acidic tide is expected. However, in the gastric trout, the kidney responded with an appropriate increase in base excretion (8). Accordingly, changes in mRNA expression for epithelial acid-base transporters, including Rhesus glycoproteins, have been observed in the gills (87) and intestine (10) of trout following feeding, but nothing is known about molecular responses in the kidney.

The present study aimed to *1*) describe the distribution of key acid-base and ammonia transporters in different parts of the nephron of the agastric goldfish, and *2*) to investigate the physiological and molecular effects of feeding on renal function with respect to acid-base and ammonia regulation. We were able to microdissect and isolate intact kidney tubule sections, which enabled us to characterize the regulation and differential expression patterns of key epithelial transporters, including Rhesus glycoproteins by the application of quantitative real-time PCR (qPCR) and immunohistochemistry (IHC) on the individual sections. Our first hypothesis was that epithelial transporters and especially Rhesus glycoproteins would be differentially expressed along the different renal tubule sections and that this pattern would strongly correlate with the mammalian system. Our second hypothesis was that changes in the expression of these transporters would occur following feeding in accord with typical responses to a metabolic acidosis seen in the mammalian nephron. We also included the urinary bladder in our qPCR analysis, because this terminal organ has the potential to fine-tune the ultimately released urine (19, 20), and, consequently, we predicted a role for this organ in acid-base and ammonia regulation.

MATERIALS AND METHODS

Animal Care

All procedures were conducted under the approval of the University of British Columbia Animal Care and Use Committee (license no. A14-0251) and the guidelines of the Canadian Council on Animal Care.

For mRNA and protein analyses, small goldfish *C. auratus* with an approximate length of ~5 cm (2.3 ± 0.1 g) were obtained from Noah's Pet Ark (Vancouver, BC, Canada) and kept in recirculating and filtered 75-liter aquaria. For physiological measurement on urine composition, bigger goldfish of ~10 cm (22.1 ± 0.7 g) were obtained from The Little Fish Company (Surrey, BC, Canada) and kept in recirculating and filtered 200-liter or 700-liter tanks in the zoology aquatic facilities of the University of British Columbia (Vancouver, BC, Canada). In all setups, fish were held in dechlorinated Vancouver tap water [in μmol/l: ~70 Na^+, 73 Cl^-, 7 Mg^{2+}, 89 Ca^{2+} (47), pH 7.13 ± 0.05] at 18°C at a light cycle of 12:12-h light-dark at a maximum density of 1 animal/3 liters. Water ammonia and pH levels were closely monitored, and water changes were performed 1–2 times per week as necessary. All fish were fed 3 times/wk at 1% of their body weight with commercial flake (small goldfish; Nutrafin Max, Hagen, Montreal, QC, Canada) or pellet food (big goldfish; 3.5-mm milling type; Ewos, Surrey, BC, Canada).

Whole Animal Nitrogenous Waste Excretion

After being fed to satiation, small goldfish were placed into individual 2-liter plastic containers and allowed to rest for 15–20 min. Following this settling period, a water sample was taken (reference = 0 h). Subsequently, 5-ml water samples were taken after 1, 2,

4, 6, 12, and 24 h and immediately frozen at −20°C until further analysis for ammonia and urea.

Spot-Sampling of Goldfish Urine

For spot-sampling of the urine, 6–8 big goldfish were transferred into individual 250-ml plastic containers with a flow-through of aerated tap water from a 200-liter reservoir 24 h before spot-sampling. All animals were starved for 96 h (control) before either being fed directly in the containers (for time points 3 h and 6 h), or in the big holding tanks immediately before transfer (for time point, 24 h). Fish were quickly anesthetized with 300 mg/l tricaine methane sulfonate (MS-222; pH neutralized with 1 M KOH) and transferred to the procedure table. After drying off any remaining water, the tip of a catheter was carefully inserted into the urogenital papilla and guided up into the bladder. The catheter was made of polyethylene (PE)-50 tubing with a narrowed end bent at a 90° angle to account for the specific anatomy of the goldfish bladder. Mild suction was applied with a 1-ml syringe to drain the urine from the bladder (typically, 8–15 μl). pH was measured at 18°C with a microelectrode (Orion PerpHecT ROSS Combination pH Micro Electrode (cat. no. 8220BNWP); Thermo Fisher Scientific, Surrey, BC, Canada) connected to a hand-held Symphony pH-meter (SP70; VWR International, Mississauga, ON, Canada) before all samples were frozen at −20°C until further analysis for total ammonia, urea, and inorganic phosphate.

Analysis of Physiological Samples

Total ammonia ($NH_3 + NH_4^+$) in all water (for whole animal excretion) and urine samples was determined colorimetrically by the sodium salicylate-hypochlorite method, as described by Verdouw et al. (71), while urea was determined by the diacetyl monoxime method of Rahmatullah and Boyde (58). Inorganic phosphate was measured by the method of Murphy and Riley (48).

Sampling for Kidney Sections mRNA

For mRNA expression under fasted conditions, animals were not fed for 96 h before being killed. For fed conditions, goldfish were fasted for 93 h, fed, and then left in the tank for additional 3 h before being killed. Each animal was quickly killed by cephalic concussion to avoid potential effects of anesthetics. The bladder (BL) with adjacent parts of the Wolffian duct running through the body cavity (hereafter referred to as "Wolffian body" or WB), as well as the whole kidney, were excised and stored in ice-cold goldfish Ringer solution containing in g/liter (mmol/liter): 5.8 (100.0) NaCl, 0.19 (2.5) KCl, 0.22 (1.5) $CaCl_2 \cdot 2H_2O$, 0.20 (1.0) $MgCl_2 \cdot 6H_2O$, 1.26 (15.0) $NaHCO_3$, and 0.07 (0.5) $NaH_2PO_4 \cdot H_2O$, according to Hoar and Hickman (29). Subsequently, the two Wolffian ducts running through the kidney (hereafter referred to as "Wolffian kidney" or WK) were dissected first by pulling apart the tubules with fine forceps and needles. CDs and connecting tubules (CT) were then carefully cut from the semi-clean Wolffian duct using the sharp edge of a 25 G × 5/8-inch needle (Becton Dickinson, Franklin Lakes, NJ). Finally, single tubules were carefully pulled out of their cluster with microdissecting insect needles, and at least 10 proximal tubule (PT) and DT sections were collected. These sections were distinguished according to Sakai (62): The thicker PT ends in a specific, distinguishable bend, after which it straightens and gradually thins out. The cut to divide PT and DT was made approximately in the middle of the straight part after this recognizable "kink" [see Sakai (62) Figs. 8 and 9; Fig. 3*A* of the present study].

For the first dissections, equally small amounts of whole kidney tissue were either immediately stored on ice in ice-cold RNAlater or ice-cold saline for the length of the dissection to check for potential degradation. We found only negligible degradation and no significant differences in total RNA levels for both treatments (data not shown) and, therefore, concluded that isolated sections were viable for a 3-h time period when kept on ice in ice-cold goldfish Ringer. As a result of these tests, a maximum time of 3 h after killing the animals was allowed to collect the sections on ice in ice-cold Ringer to avoid degradation of the RNA.

Quantitative Real-Time PCR

Immediately after dissection, total RNA of each kidney section was extracted with the RNAqueous-Micro total RNA isolation kit (Ambion, Thermo Fisher Scientific, Pittsburgh, PA). Total RNA was then treated with DNase I (Invitrogen, Thermo Fisher Scientific, Carlsbad, CA) to eliminate DNA traces and was quantified by Nanodrop analysis. Regular PCR on the elongation factor 1α [EF1α; forward: TTTCACCCTGGGAGTCAAAC, reverse: TCTTCCATCCCTTGAACCAG (39)] was performed to ensure successful treatment. Maximum available amounts for each section of verified clean RNA (tubule sections PT/DT/CT/CD = 2.1 ± 0.2 ng, WK/WB/BL = 4.9 ± 0.1 ng) was then transcribed to cDNA with the iScript cDNA synthesis kit (Bio-Rad, Mississauga, ON, Canada). For whole kidney samples, total RNA was extracted using TRIzol (Invitrogen) and 0.9 μg was treated with DNase I, checked for successful treatment, and transcribed as described above.

Each qPCR reaction was set up in a total volume of 15 μl, containing 0.4 pmol primer, 2 μl cDNA, and 7.5 μl SsoFast EvaGreen Supermix (Bio-Rad, Hercules, CA). The reactions were run in 96-well plates on a Bio-Rad CFX connect cycler, and runs were analyzed using the Bio-Rad CFX manager 3.1 software (Mississauga, ON, Canada). For each run, cDNA was denatured for 2 min at 98°C, followed by 40 cycles of 5 s at 98°C and 20 s at 60°C for annealing. A melt curve analysis from 65°C to 95°C in 1°C increments was run to verify single amplicons. For absolute quantification, a standard curve based on a 1:1 serial dilution of a cDNA-mix of kidney tubule sections was included for each gene (efficiency = 95–105%, $R^2 \geq 0.98$). Goldfish gene-specific primers for elongation factor 1α (EF1α), V-H^+-HAT, subunit 1b (HAT1b), Na^+/K^+-ATPase subunit 1α (NKA1α), and Rhesus protein isoform-bg (Rhbg), -cg1a (Rhcg1a), and -cg1b (Rhcg1b) were used as described by Lawrence et al. (39) and Sinha et al. (66), while primers for NHE3, carbonic anhydrase II (CAIIa), Na^+/HCO_3^--cotransporter isoform 1 (NBC1), anion exchanger Cl^-/HCO_3^- isoform 1 (AE1), glutamate dehydrogenase (GDH), glutamine synthetase (GS), aspartate aminotransferase mitochondrial (ASP-ATm), aspartate aminotransferase cytoplasmic (ASP-ATc), and alanine aminotransferase (ALA-AT) were newly designed (details and accession numbers are given in Table 1). Ef1α mRNA expression did not change significantly between fasted and fed animals (data not shown) and was consequently used as the reference gene for internal normalization. Data are displayed as gene/EF1α ratio.

Protein Expression Analyses

Western blot analysis. Whole goldfish kidneys were isolated on ice, homogenized in buffer [50 mmol/l Tris (pH 8.0), 50 mmol/l NaCl, 1% Triton-X 100, protease inhibitor cocktail (Calbiochem, San Diego, CA)] and centrifuged for 5 min at 4°C at 13,000 *g*. Supernatants were sonicated on ice for 1 min (3 × 10-s pulses with 10-s pauses) and centrifuged again as described above. Protein content was determined applying the BCA method using the Pierce BCA protein assay kit (Thermo Fisher Scientific). Supernatants were then pooled and mixed 1:6 with 6× Lämmli's running buffer. After heating samples to 95°C for 7 min and centrifuging for 7 min at 13,000 *g*, 200 μg protein was loaded into the lanes of two Lonza PAGEr EX gel (4–12%; Lonza, Basel, Switzerland) for PAGE using the Hoefer VE chamber (Holliston, ME). PAGE gels were run at 200 V in 0.67× Lonza ProSieve EX running buffer. Gels were then transferred onto PVDF membranes (Bio-Rad) soaked in methanol and transfer buffer at 30 V using a semidry blotting apparatus (Hoefer TE70X) and 1× ProSieve EX

Table 1. *Primer information for qPCR*

Gene	Source(s)/Reference	Primer Sequence	Amplicon Length, bp
EF1α	AB056104.1/(39)	F: TTTCACCCTGGGAGTCAAAC R: TCTTCCATCCCTTGAACCAG	227
NHE3	JZ545951.1/this study	F: GCCATTCTCATTTACGCCAT R: AGACCGATGTCCAAGTCACC	110
HAT1b	JX570886.1/(66)	F: CTATGGGGGTCAACATGGAG R: CCAACACGTGCTTCTCACAC	186
CAIIa	NM_199215.1, AB055617.1/this study	F: CTCCATCTGGTCCACTGGAA R: ATAGCATCCATAGCATCCAG	146
NBC	AB055467.1, NM_001124325.1, EF634453.1/this study	F: GCCGTCATGTTAGGAGGTCT R: CACGGTATGACTTGGCCTTT	94
AE	NM_001168266.1/this study	F: CACAATTCATCCTGATGGCA R: ACAGCCAAACATAAGGCACA	100
NKA1a	JX570887.1/(66)	F: GTCATGGGTCGTATTGCATC R: GTTACAGTGGCAGGGAGACC	227
Rhbg	JX570883.1/(66)	F: ATGATGAAACGGATGCCAAG R: TCCTGGAAACTGGGATAACG	103
Rhcg 1a (a, 1)	JX570884.1/(66)	F: GCTGGTTCCATTCTCTGGAC R: ATCTTCGGCATGGAGGACAG	209
Rhcg 1b (b, 2)	JX570885.1/(66)	F: ATTGTGGGCTTCTTCTGTGG R: GGCACACGTTTCTCAAAAGC	239
GS	AY641442.1/this study	F: CTGCCTCTATGCTGGTGTGA R: GATCTCCCATGTTGATGCCT	104
GDH	JN634757.1/this study	F: CCAAATTTCCCTCTGCAAAA R: GGAAATGGGGTTAGGCTGAT	107
ASP-ATm	AB793727.1/this study	F: TGGATCTCTTCGTGTTGGTG R: TCTCTGAAGATAGGGGTGTGG	108
ASP-ATc	NM_213057.2/this study	F: TCGGAGCCTACAGGACAGAT R: AGAATGGGCAGGTACTCGTG	112
ALA-AT	NM_001098757.2/this study	F: TCAGTACCCGCTTTACTCTGC R: AAGTTCGTTGATGTCCAGGG	103

Sources are accession numbers as obtained from NCBI. bp, base pair; F, forward; R, reverse.

Western blot transfer buffer (Lonza, Basel, Switzerland). Subsequently, membranes were stained with Ponceau S to ensure proper transfer of the proteins. Membranes were photographed, lanes were clearly and individually marked with reference to the protein marker and cut into single lanes before being destained to be incubated with the suite of antibodies (1 antibody/lane), as described in Table 2. Membrane parts were blocked for 30 min in 5% skim milk in Tris-buffered saline containing Tween-20 (TBS-T) and individually incubated with the respective first antibodies overnight at 4°C. Following incubation with the first antibody, membranes were washed 3× with TBS-T and incubated with the second antibody (HRP-conjugated goat anti-rabbit (Invitrogen); 1:50,000) for 1 h at room temperature. To visualize signals, individual membrane strips were reassembled with reference to their marker using the respective markings as described above and probed with SuperSignal WEST Femto Maximum Substrate (Thermo Fisher Scientific) before being scanned with the Imager VersaDoc MP4000 (Bio-Rad).

Preparation of whole-mount tubule sections for immunohistochemistry. Kidney tubules were dissected as described earlier for the preparation of mRNA but were kept at whole length instead of being divided into sections. Dissection of the first half kidney was limited to 1 h, after which tubules were stored in the fridge for maximum 1 h and/or until the second half was dissected. Tubules were collected in TBS-T, fixed in 4% paraformaldehyde for 10 min, and then washed 3× for 10–15 min with TBS-T. Permeabilization of the tubules was increased by incubation in TBS-Triton-X 100 for 30 min. After blocking the tissues with 1% BSA in TBS-T for 45 min, tubules were transferred onto individual microscope slides and incubated with the respective first antibody in 1% BSA/TBS-T (see Table 2) overnight at 4°C in wet chambers. The following day, tubules were washed 3× for 10–15 min with TBS-T before being incubated with the second antibody (goat anti-rabbit Alexa Fluor-546 conjugated; Invitrogen) in 1% BSA/TBS-T for 1 h at room temperature. After repeated washing (3× TBS-T for 10–15 min), nuclei were stained with DAPI for 10

Table 2. *Antibody information*

Target Gene	Antibody Name/Species	Dilution IHC	Dilution Western	Expected Size*	Reference	Courtesy of
NHE3	NHE3R18/*Oncorhynchus mykiss*	1:200	1:500	110	(30, 31, 86)	Dr. S. Perry
HAT1b	B1/*Anguilla anguilla*	1:200	1:1,000	56	(78, 86)	Dr. J. Wilson
CAIIa	CA2/*Homo sapiens*	1:100	1:5,000	30	(86)	(Abcam ab191343)
NKA1α	αR1/*Oncorhynchus masou*	1:200	1:5,000	100/50	(70, 78, 86)	Dr. J. Wilson
AE1	tAE1/*Tilapia sp.*	1:100	1:2,000	110	(67)	Dr. P. P. Hwang
NBC1	NBCe1/*Takifugu obscurus*	1:1,000	1:1,000	120–140	(37)	Dr. S. Hirose/Dr. N. Nakamura
Rhbg	fRhbg/*Takifugu rubripes*	1:500	1:5,000	47	(51, 52)	Dr. S. Hirose/Dr. N. Nakamura
Rhcg1a	drRhcg1/*Danio rerio*	1:1,000	1:500	39	(50, 52, 86)	Dr. S. Hirose/Dr. N. Nakamura
Rhcg1b	fRhcg2/*Takifugu rubripes*	1:100	1:5,000	47	(51, 52)	Dr. S. Hirose/Dr. N. Nakamura

*Based on reference paper and/or *Cyprinus carpio* sequence. IHC, immunohistochemistry.

min, and slides were mounted in Mowiol/DABCO. All pictures were taken with the Olympus FV1000 Confocal of the UBC Bioimaging Facility the day after staining, with the exact same settings that had previously been established and optimized for each antibody. For the purposes of immunohistochemistry (IHC), only three major segments of the nephron (PT, DT, and CT) were examined.

Analysis of IHC for protein expression levels. Protein expression levels for all genes of interest were semiquantified from the pictures taken at the confocal. Applying the software Fiji (63)/ImageJ (59), representative areas of ≥5 adjacent cells were chosen for both membranes of the tubule in each photo. Cells were counted and their area was determined, using units of both pixels and micrometers, as well as the fluorescence intensity of the protein of interest. Protein expression levels are represented as total fluorescence per cell (cell fluorescence = cell area × average fluorescence intensity) according to Wilson et al. (78), and compared between fasted and fed animals, as done for mRNA levels.

Statistics

All statistical analyses were performed in PAST3 (26). Data were checked for normal distribution (Shapiro-Wilk Test) and homogeneity of variances (*F*-test) before testing. If a data set did not pass these criteria for parametric testing, it was log transformed. For the comparisons of two means, Student's *t*-test was applied (mRNA and protein expression), while ANOVA with Tukey's post hoc test was applied for the comparison of multiple means (urine sampling). All values are expressed as means ± SE. For whole animal excretion rates, the ANOVA was based on repeated measures. All data graphs were generated using Excel and Inkscape 0.92.0 r15299 (https://www.inkscape.org). Photos of Fig. 3 were edited in Photoshop 6.0 by blacking out the background and increasing the contrast. Photos of Figs. 7 and 8 were edited in Fiji (63) and ImageJ (59) by increasing overall brightness and contrast.

RESULTS

Effect of Feeding on the Excretion of Nitrogenous Waste

The whole animal excretion rate of total ammonia (NH_3 + NH_4^+) significantly increased three-fold from 0.64 ± 0.09 μmol·g^{-1}·h^{-1} to 1.89 ± 0.19 μmol·g^{-1}·h^{-1} only 1–2 h after feeding (Fig. 1*A*) and stayed elevated for another 2–4 h. After 6–12 h, total ammonia excretion decreased back to control levels. Urine total ammonia levels were significantly increased only after 6 h from 0.54 ± 0.12 mmol/l to 1.24 ± 0.23 mmol/l (Fig. 2*A*). While whole animal urea excretion increased 6-fold within the first hour after feeding (0.07 ± 0.01 μmol g^{-1} h^{-1} to 0.40 ± 0.11 μmol g^{-1} h^{-1}), it dropped back to control levels after 2–4 h and then rose back up after 4–6 h (Fig. 1*B*). No changes in urea concentrations in the urine occurred in that same time frame. However, at 24 h after feeding, urine urea levels decreased by ~50% from 0.77 ± 0.12 mmol/l to 0.36 ± 0.11 mmol/l (Fig. 2*B*). In contrast to the delayed elevation of urine total ammonia concentration, urine pH dropped by 0.6 units at 3 h after feeding (Fig. 2*C*) in parallel to a significant fourfold rise in inorganic phosphate from 0.54 ± 0.11 mmol/l to 2.10 ± 0.56 mmol/l (Fig. 2*D*).

Morphology of Kidney Tubule Sections

Generally, the morphology of the whole goldfish kidney did not resemble the mammalian organization into the cortex and medulla and seemed much more unstructured. The different sections of the microdissected renal tubules could clearly be distinguished into the wider PT and a narrower DT when teased apart (Fig. 3*A*). The late DTs then widened out again into what has previously been described as CTs by Sakai (62). Multiple CTs then joined together to form the CDs that entered the Wolffian duct (W_K) at a 90° angle (Fig. 3*B*). Interestingly, more kidney-like tubules (TB) could be observed between both Wolffian ducts (W_B) shortly before they united to form the bladder (BL, Fig. 3*C*). Even though a clear pattern could not be established, many glomeruli seemed to be in contact with either a neighboring tubule or folding back onto their own earlier tubule, often close to the region where the PT transformed into the DT (Fig. 3, *D* and *E*).

mRNA Expression Patterns and the Effect of Feeding on mRNA Levels in Whole Kidney

Whole kidney–epithelial transporters. Throughout the whole kidney, average mRNA expression levels in fasted goldfish were at a similar level (0.7–1.1 arbitrary units, AU) for most investigated transporters, except for a ~50% lower expression (0.3 ± 0.1 AU) of anion exchanger 1 (AE1), while Rhesus-glycoprotein cg1b (Rhcg1b) was not detectable (Fig. 4*A*). In response to feeding, Rhcg1b mRNA expression increased to a mean level comparable to the other transporters (1.0 ± 0.6 AU). It was still not detectable in all fed animals,

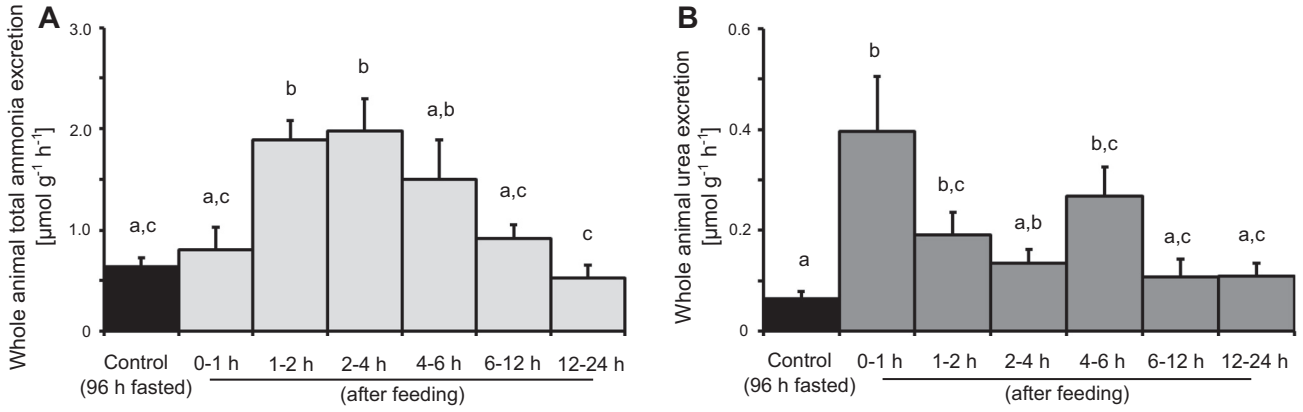

Fig. 1. Time course of whole animal nitrogenous waste excretion of goldfish after feeding. Total ammonia (NH_3+NH_4^+) excretion rates (*A*) and urea excretion rates (*B*). Means not sharing the same lowercase letter are significantly different from one another (repeated-measures ANOVA with Tukey post hoc analysis, $P < 0.05$). All values are displayed as means ± SE; $n = 5–8$.

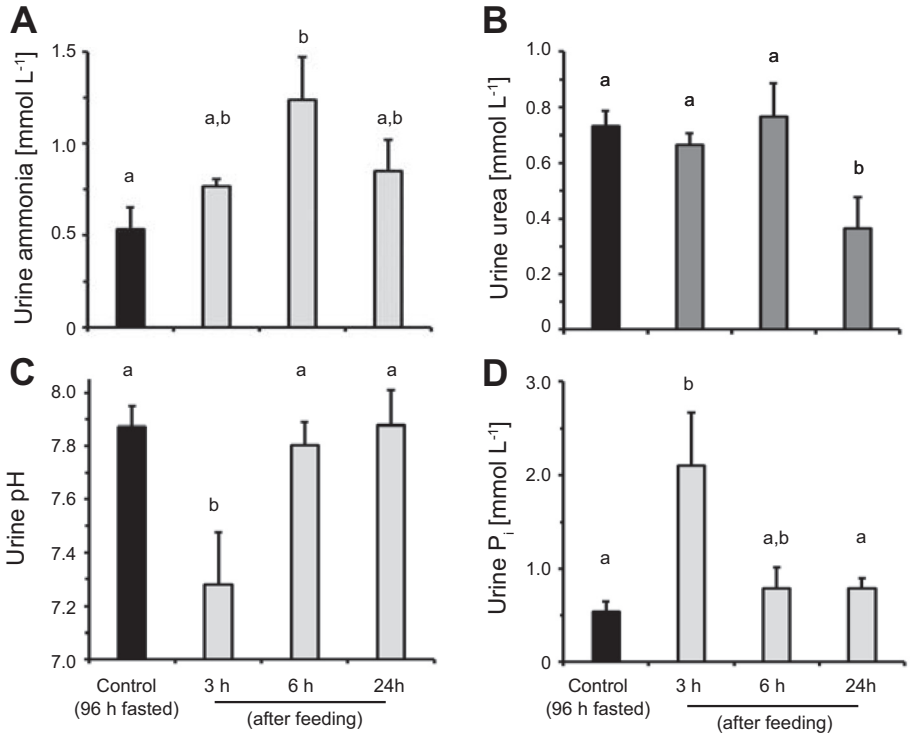

Fig. 2. Indicators for urinary acid- and N-waste excretion by the goldfish kidney after feeding. total ammonia ($NH_3+NH_4^+$) concentration (*A*), urea concentration (*B*), urine pH (*C*), and inorganic phosphate (*D*) concentration. Means not sharing the same lowercase letter are significantly different from one another (ANOVA with Tukey post hoc analysis, $P < 0.05$). All values are displayed as means ± SE; $n = 5$–15.

however, so that the level of upregulation was highly variable and, hence, not statistically significant ($P = 0.08$). The only significant response upon feeding was observed for Na^+/H^+-exchanger 3 (twofold upregulation from 0.77 ± 0.16 to 1.54 ± 0.32 AU).

Whole kidney–enzymes involved in ammoniagenesis. With the exception of a lower expression level of glutamate dehydrogenase (GDH; 1.1 AU), mRNA for all investigated enzymes potentially involved in the generation of ammonia-glutamine synthetase (GS), aspartate aminotransferase (ASP-AT (mitochondrial and cytoplasmic), and alanine aminotransferase (ALA-AT) was expressed to a similar level in fasted goldfish (3.2–3.6 AU) (Fig. 4*B*). Upon feeding, GS mRNA exhibited a decrease to 1.5 ± 0.3 AU ($P = 0.07$), while mRNA expression of GDH was significantly increased to a level comparable to that observed for the other enzymes in fasted goldfish (3.2 ± 0.6 AU).

Section-Specific mRNA Expression Patterns and the Effect of Feeding on mRNA Levels in the Nephron

General observations for mRNA expression of epithelial transporters in distinct kidney sections. Profiling of mRNA expression in different tubule sections (Fig. 5) revealed a far more heterogeneous pattern, and a far greater number of specific changes in the mRNA expression patterns associated with feeding than seen in the whole kidney (Fig. 4). In fasting goldfish, most of the investigated genes seemed to have a unique mRNA expression pattern throughout the different tubule sections and the bladder, suggesting a different functional role for each part. The only exceptions were the V-H^+-ATPase subunit 1b (HAT1b) and the anion exchanger 1 (AE1) with a similar and overall relatively low, but homogenous expression profile (Fig. 5, *B* and *E*). Overall high and fairly similar levels of mRNA expression were detected for the Na^+/H^+-exchanger (NHE3, CT, and CD; Fig. 5*A*), carbonic anhydrase (CAIIa, CT, and CD; Fig. 5*C*), Rhesus glycoprotein bg (Rhbg, DT; Fig. 5*G*), and Rhesus glycoprotein cg1a (Rhcg1a, CT; Fig. 5*H*).

Upon feeding, however, the DT seemed to play an increased role as evidenced by the upregulation of various transporters (NHE3, HAT1b, CAIIa, and Rhcg1b) and the downregulation of Rhbg. Generally, in response to feeding, two of the three Rhesus glycoproteins (Rhbg and Rhcg1b; Fig. 5, *G* and *I*) underwent the most marked changes in mRNA expression levels beside the prominent downregulation of Na^+/HCO_3^--cotransporter in the bladder (Fig. 5*D*).

Na^+/H^+-exchanger. In fasted goldfish, the highest expression of mRNA for Na^+/H^+-exchanger (NHE3) was observed in the CT and CD (Fig. 5*A*). The level of expression here was higher than for any of the other genes in any of the other tubule sections. Upon feeding, expression was significantly increased in proximal (PT; 40-fold from 0.06 ± 0.02 to 2.39 ± 0.48 AU) and DT (6.4-fold from 0.21 ± 0.06 to 1.35 ± 0.28 AU), as well as bladder (12-fold from 0.02 ± 0.01 to 0.24 ± 0.13 AU), while NHE3 was expressed only at very low levels in these sections in fasted conditions. NHE3 was also expressed in both parts of the Wolffian duct (W_K and W_B), but did not respond to feeding in this part of the kidney.

V-H^+-ATPase, subunit 1b. The level of mRNA expression of V-H^+-ATPase, subunit 1b (HAT1b) was generally relatively low and homogenous in all kidney tubule sections and bladder, both in fed and fasted animals (Fig. 5*B*). While there seemed to be a general trend for HAT1b to be upregulated in the PT and DT in response to feeding, with a significant twofold increase in the DT from 0.13 ± 0.02 to 0.26 ± 0.05 AU, its overall level of change was small in comparison to changes in other genes.

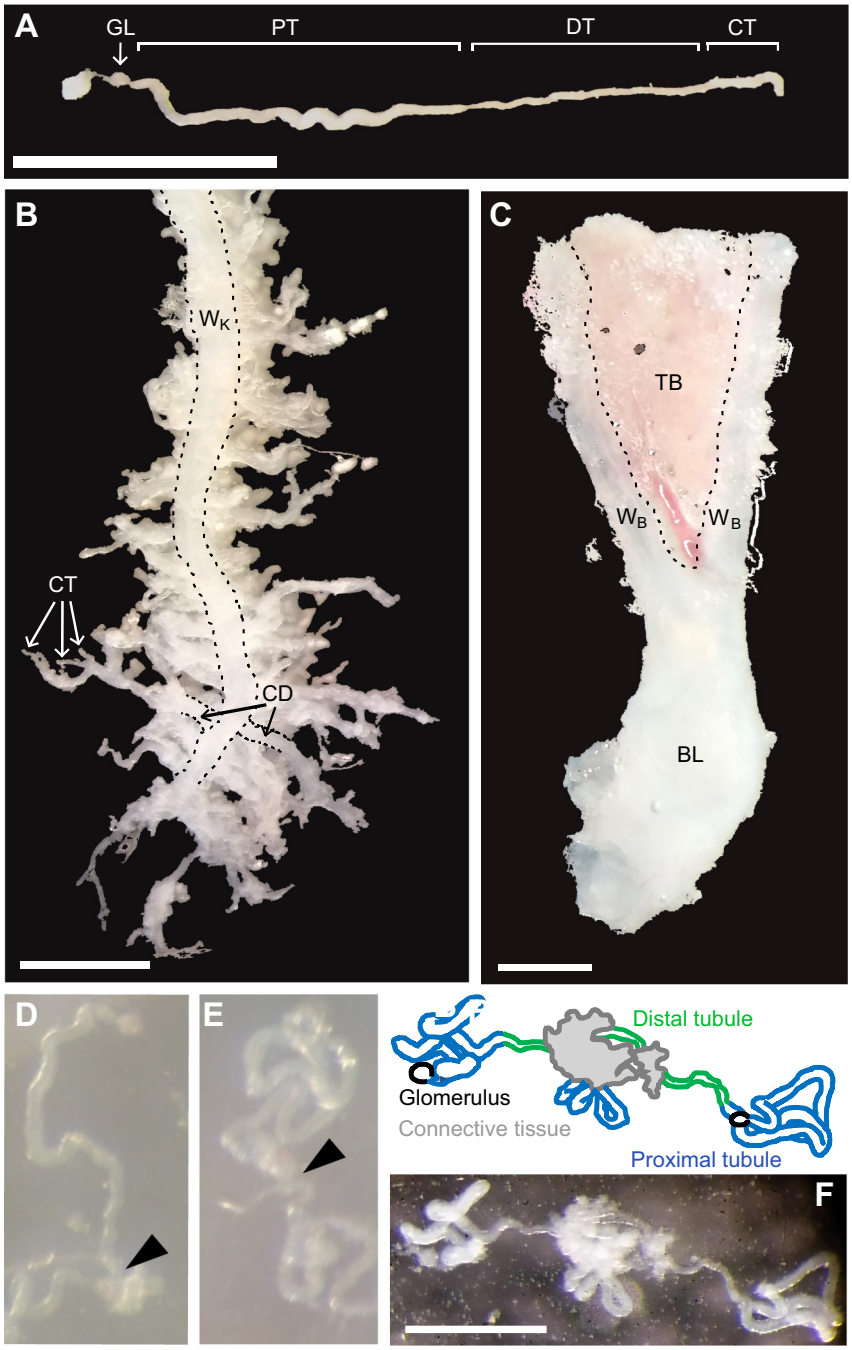

Fig. 3. Morphology of investigated components of the goldfish (*Carassius auratus*) kidney. *A*: isolated renal tubule. *B*: one isolated Wolffian duct as it runs through one half of the kidney branching into collecting ducts at ~90° angles. *C*: paired Wolffian ducts fusing caudally into the bladder. Glomeruli from the same or another tubule often seem to be attached to the distal tubule (*D*), and/or to the region where the proximal leads into the distal tubule (*E*), as indicated by the black triangles. *F*: distal and connecting tubules are usually observed to be densely covered in connective tissue to form potential functional units (photo and cartoon). BL, bladder; CD, collecting duct; CT, connecting tubule; DT, distal tubule; GL, glomerulus; PT, proximal tubule; TB, tubules associated with bladder; W_B, Wolffian duct as it runs through the body; W_K, Wolffian duct as it runs through the kidney. Scale bars: 1 mm.

Carbonic anhydrase IIa. In fasted animals, CAIIa (Fig. 5*C*) was present in all kidney tubule sections, but was less expressed in the two parts of the Wolffian duct and bladder. Highest mRNA expression in fasted animals was observed in the CT and CD. Interestingly, the high levels in CT and CD were downregulated upon feeding (from 3.19 ± 0.32 to 2.12 ± 0.18 and 2.97 ± 0.47 to 1.72 ± 0.15 AU, respectively), whereas CAIIa in the DT was twofold upregulated (from 1.11 ± 0.15 to 2.19 ± 0.38 AU). As a result, CAIIa levels in these three sections were very similar in fed animals, but still approximately twofold higher than in all PTs, Wolffian ducts, and bladder.

Na^+/HCO_3^--cotransporter 1. In fasted as well as fed animals, Na^+/HCO_3^--cotransporter 1 (NBC1) mRNA was mainly expressed in the two parts of the Wolffian duct, as well as in the bladder in fasted goldfish only (Fig. 5*D*). Expression levels in the PT, DT, and CT were negligible. mRNA expression in the CD was at an intermediate level. Upon feeding, NBC1 was significantly downregulated (by 87.5%, from 1.12 ± 0.36 to 0.14 ± 0.07 AU) in the bladder. The expression pattern was opposite to those of NHE3 (cf. Fig. 5*A*), as well as CAIIa mRNA (cf. Fig. 5*C*) throughout the different sections.

Cl^-/HCO_3^--anion exchanger 1. Similar to HAT1b (cf. Fig. 5*B*), anion exchanger 1 (AE1; Fig. 5*E*) mRNA was evenly

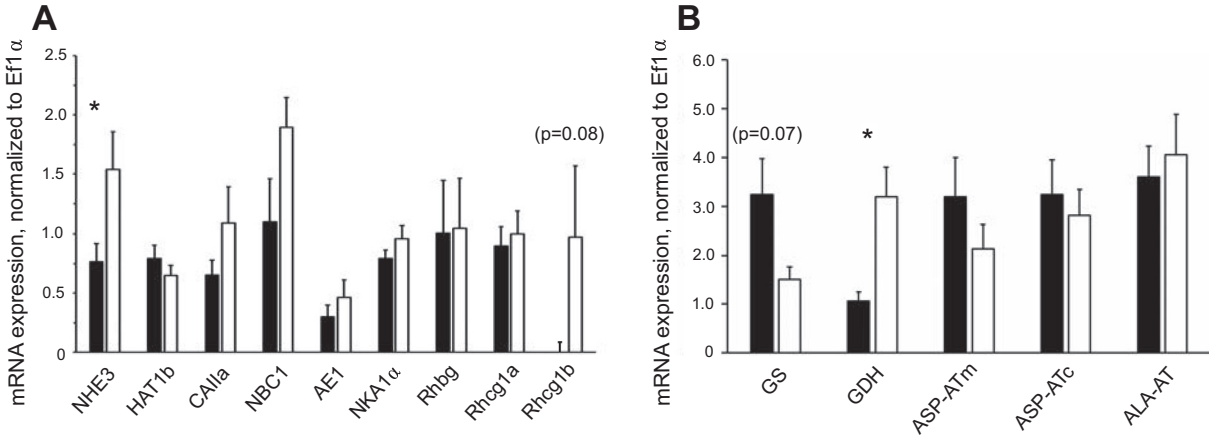

Fig. 4. Changes in mRNA expression of epithelial transporters relevant for acid-base and ammonia balance in the whole kidney in response to feeding. *A*: epithelial transporters: NHE3, Na^+/H^+-exchanger isoform 3; HAT, V-H^+-ATPase subunit 1b; CAIIa, carbonic anhydrase isoform IIa; NBC1, Na^+/HCO_3^--cotransporter isoform 1; AE1, anion exchanger 1; and NKA1α, Na^+/K^+-ATPase α-subunit. *B*: enzymes involved in generation of ammonia: GS, glutamine synthetase; GDH, glutamate dehydrogenase; ASP-ATm, aspartate aminotransferase mitochondrial; ASP-ATc, aspartate aminotransferase cytoplasmic; ALA-AT, alanine aminotransferase. *Significant differences between fasted (96 h; black bars) and fed (3 h after feeding; open bars) goldfish (Student's *t*-test, $P < 0.05$). Values are expressed as means ± SE; $n = 4–6$.

expressed throughout all tubule sections and the bladder at a relatively low level in both fasted and fed animals. Even though there seemed to be a tendency for AE1 to be upregulated in fed vs. fasted goldfish (DT, CT, and bladder), the changes were not significant.

Na^+/K^+-ATPase subunit 1α. Interestingly, NKA1α (Fig. 5*F*) mRNA could not be detected in PT and DT and was hardly present in the bladder in either fasted or fed animals. mRNA expression in all other sections was high and at a similar level. However, it did not change with feeding.

Rhesus glycoprotein b. In fasted goldfish, the highest level of Rhesus glycoprotein b (Rhbg) (Fig. 5*G*) mRNA expression was observed in the DT. While PTs still had modest amounts of Rhbg mRNA, the remaining sections exhibited only very low expression levels of the mRNA for this channel. Upon feeding, a mixed response was observed with a significant 50% downregulation in the DT (from 5.02 ± 0.82 to 2.50 ± 0.30 AU), but 24-fold upregulation (from 0.10 ± 0.05 to 2.38 ± 0.70 AU) and 14-fold upregulation (from 0.28 ± 0.10 to 4.05 ± 1.59 AU) in CT and CD. The direction of these responses in Rhbg was exactly opposite to those observed for CAIIa in those sections (cf. Fig. 5*C*), but, interestingly, as a result of these adjustments, the overall expression pattern was then strikingly similar between the two in fed goldfish.

Rhesus glycoprotein c, isoform 1a. With low levels of mRNA expression in PT and DT, highest expression in CT and duct, and no detectable expression in the bladder, the profile of Rhesus glycoprotein c, isoform 1a (Rhcg1a; Fig. 5*H*) in fasted animals was strikingly similar to that of NHE3 (cf. Fig. 5*A*). This gene, however, hardly responded to feeding and was only slightly downregulated in the Wolffian duct as it runs through the kidney.

Rhesus glycoprotein c, isoform 1b. Interestingly, Rhesus glycoprotein c, isoform 1b (Rhcg1b) mRNA expression was only detectable in the two parts of the Wolffian ducts of fasted animals (Fig. 5*I*). Upon feeding, however, mRNA expression was present at a low level in DT, as well as the bladder, and exhibited an immense upregulation to 3.08 AU in the CT and to 1.89 AU in the CD. Consequently, in fed animals, the mRNA expression pattern of Rhcg1b was very similar to the expression pattern of Rhcg1a (cf. Fig. 5*H*).

Glutamine synthetase and glutamate dehydrogenase. Unfortunately, only very limited amounts of cDNA of the generated set of kidney tubule sections were available for most sections, and only two replicates were left for PT, DT, and CT to investigate expression patterns for enzymes potentially involved in ammoniagenesis. In fasted goldfish, mRNA expression levels for both GS (Fig. 6*A*) and GDH were higher in the PT compared with the other tubule sections (Fig. 6*B*). In response to feeding, a general trend for downregulation of GS and the opposite trend of upregulation of GDH could be observed in all sections. Expression levels were very low in the CD, Wolffian duct (kidney and body) and bladder, but both enzymes showed the same significant changes in these sections as they did in the earlier ones, respectively.

Antibody Evaluation

Western blot analysis verified specific binding for each antibody of Table 2 in whole kidneys of *C. auratus*. Signals were detected for Na^+/H^+-exchanger 3 (NHE3/NHE3R18) at 115 kDa, carbonic anhydrase IIa (CAIIa/CA2) at 33 kDa, V-H^+-ATPase subunit 1b (HAT1b/B1) at 56 kDa, Na^+/HCO_3^--cotransporter isoform 1 (NBC/NBCe1) at 45 kDa, anion exchanger 1 (AE1/tAE1) at 55 kDa, Na^+/K^+-ATPase α-subunit (NKA1α/αR1) at 50 kDa, Rhesus protein isoform cg1b (Rhcg1b/fRhcg2) at 45 kDa, Rhesus protein isoform cg1a (Rhcg1a/drRhcg1) at 43 kDa, and Rhesus protein isoform bg (Rhbg/fRhbg) at 54 kDa. For NKA1α, NBC1, and AE1, antibodies were also tested on gill tissue and signals were detected at 100 kDa (NKA1α) and 135 kDa (AE1 and NBC1), respectively.

Most antibodies detected the respective proteins at their expected sizes as stated in Table 2. Minor discrepancies in observed protein sizes for NHE3, CAIIa, HAT1b, Rhcg2, Rhcg1, and Rhbg with regard to the cited literature can be explained by different running/buffer conditions of/in the gels,

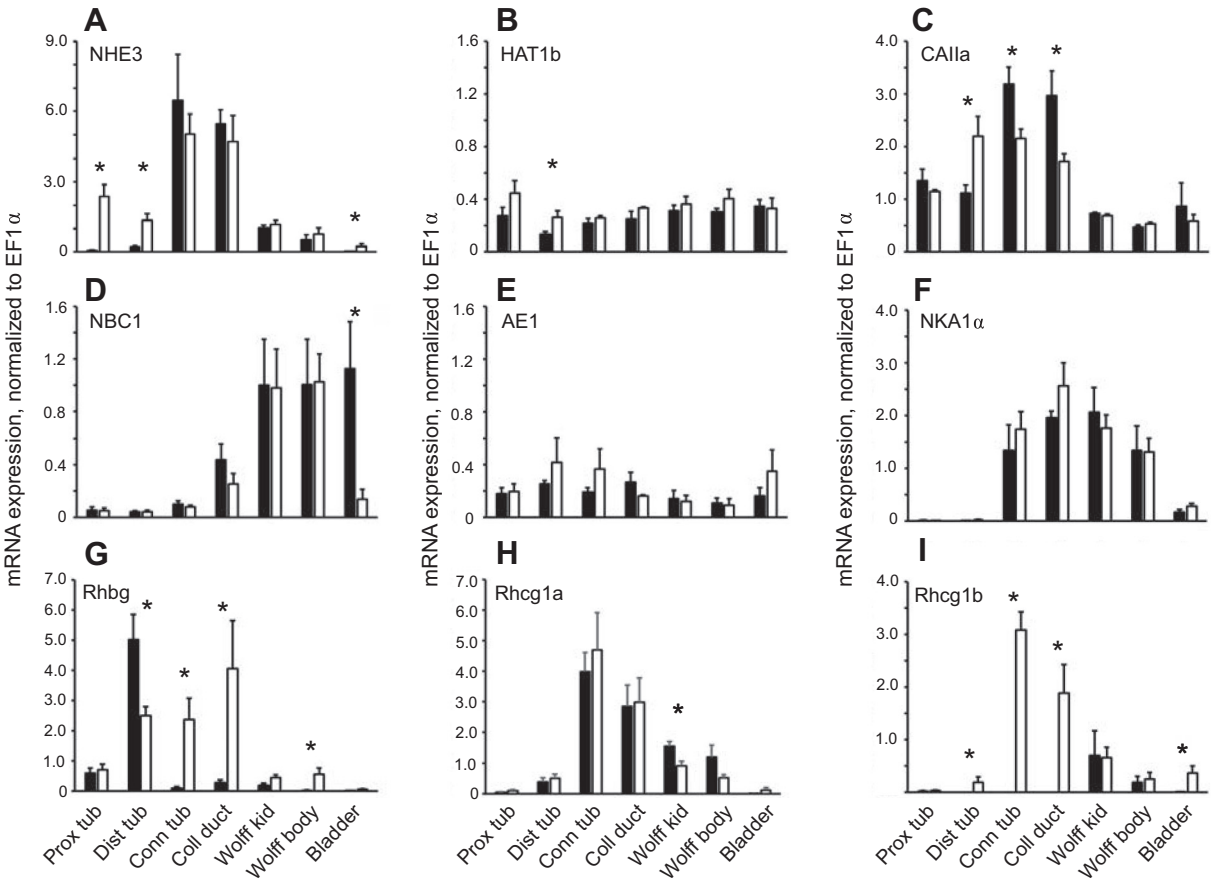

Fig. 5. Profile of mRNA expression of epithelial transporters relevant for acid-base and ammonia balance in the different kidney tubule sections, and their responses to feeding. *A*: Na^+/H^+-exchanger isoform 3. *B*: V-H^+-ATPase subunit 1b. *C*: carbonic anhydrase isoform IIa. *D*: Na^+/HCO_3^--cotransporter isoform 1. *E*: anion exchanger 1. *F*: Na^+/K^+-ATPase α-subunit. *G*: Rhesus protein isoform bg. *H*: Rhesus protein isoform cg1a. *I*: Rhesus protein isoform cg1b. *Significant differences between fasted (96 h; black bars) and fed (3 h after feeding; open bars) goldfish (Student's *t*-test, $P < 0.05$). Values are expressed as means ± SE; $n = 4–6$. Note the different scales for *A* vs. *B*, *D*, *E* vs. *C*, *F*, *I* vs. *G*, *H*.

subjectivity in reading the sizes off the gel, and the fact that some of these proteins have, indeed, slightly different amino acid compositions in different fish species, which might result in slightly different protein confirmations and/or states of glycosylation. In the cases of NKA1α, NBC1, and AE1, however, even though the correct protein size was detected in gill, the detected proteins appeared smaller in the kidney than referenced to in the literature (37, 67). This phenomenon corresponds to findings by Ura et al. (70) for NKA in Masu salmon gill vs. kidney. Having detected distinct single signals

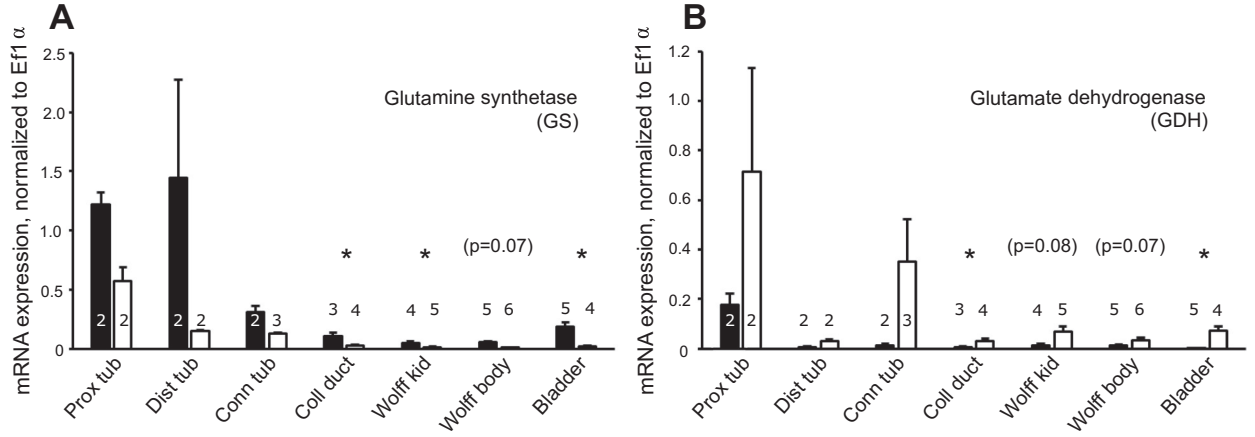

Fig. 6. Profile of mRNA expression of enzymes involved in the generation of ammonia in the different tubule sections and their responses to feeding. Glutamine synthetase (GS; *A*) and glutamate dehydrogenase (GDH; *B*). *Significant differences between fasted (96 h; black bars) and fed (3 h after feeding; open bars) goldfish (Student's *t*-test, $P < 0.05$ for sections with $n \geq 3$). Values are expressed as means ± SE with replicate numbers as indicated in the graph.

for the antibodies in the kidney, however, verifies their specificity also in this tissue.

Section-Specific Protein Expression by IHC and the Effect of Feeding on Protein Expression in the Nephron

In whole mounted renal kidney tubules of fasted *C. auratus* (Fig. 7*A*), NHE3 fluorescent staining was detected basolaterally in proximal and distal tubules but seemed more dispersed in connecting tubules. HAT1b (antibody name: B1) staining was restricted to the basal membrane in all three sections PT, DT, and CT. CAIIa (antibody name: CA2) protein appeared to be present in the cytosol (potentially vesicular) as indicated by a more grainy and patchy staining pattern that seemed to be more concentrated toward the basolateral membrane in PT and CT but not in DT. NBC1 (antibody name: NBCe1) signal was detected in basolateral membranes of PT, DT, and CT, while AE1 (antibody name: tAE1) was observed to be more restricted only to the basal membrane of all three sections, similar to HAT1b. NKA1α (antibody name: αR1) protein was present in the basal membrane of PT and seemed more basolaterally expressed in DT and CT. While Rhbg (antibody name: fRhbg) protein expression was restricted to the basolateral membranes of PT, DT, and CT, Rhcg1a (antibody name: drRhcg1) seemed to be present in both apical and basolateral membranes and/or intracellularly in all three sections, and Rhcg1b (antibody name: fRhcg2) was clearly expressed only in apical membranes.

In fed goldfish tubules (Fig. 8*A*), localization for most proteins was identical to their expression in fasted tubules, except for NHE3, CAIIa, and Rhbg. In PT of fed animals, NHE3 switched from the basolateral membrane to the apical membrane, while its dispersed pattern observed in CT of fasted animals changed to a more distinct basolateral signal. CAIIa protein expression was more dispersed in PT of fed

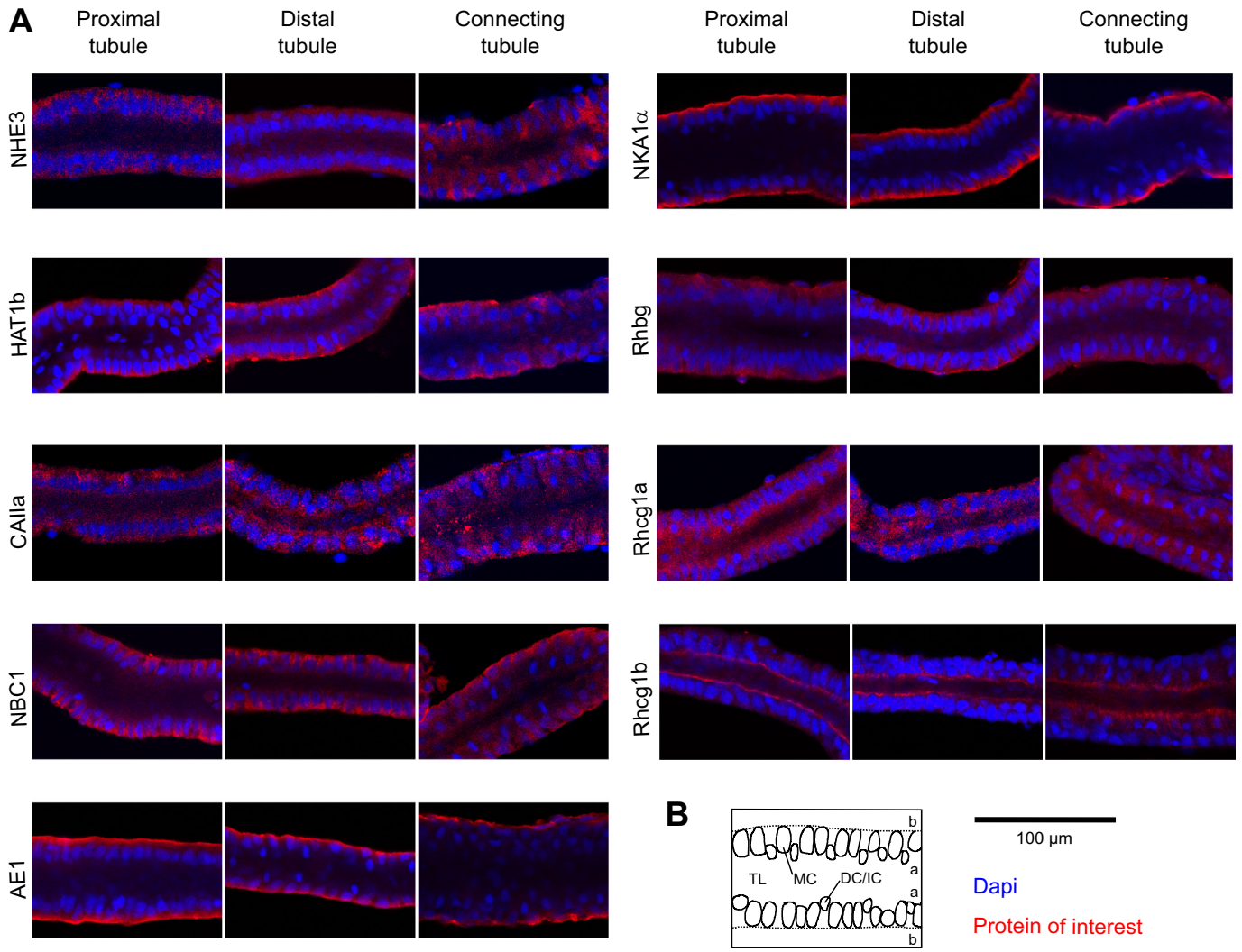

Fig. 7. Localization of proteins of interests (POI) along the kidney tubule of fasted goldfish. Immunohistochemical detection of proteins in whole-mounted proximal, distal, and connecting tubules of *Carassius auratus* kidney after 96 h of fasting. *A*: antibodies for Na^+/H^+-exchanger isoform 3 (NHE3), V-H^+-ATPase subunit 1b (HAT1b), carbonic anhydrase isoform IIa (CAIIa), Na^+/HCO_3^--cotransporter isoform 1 (NBC1), anion exchanger 1 (AE1), Na^+/K^+-ATPase α-subunit (NKA1α), Rhesus protein isoform bg (Rhbg), Rhesus protein isoform cg1a (Rhcg1a), and Rhesus protein isoform cg1b (Rhc1b), as described in Table 2. Cell nuclei were stained with DAPI (blue) and POIs with Alexa Fluor-546 (red). *B*: schematic drawing of points of interest after Sakai (62). *a*: apical; *b*: basal; DC, dark cell (in proximal and distal tubule); IC, interjacent cell (in connecting tubule); MC, main cell; TL, tubule lumen.

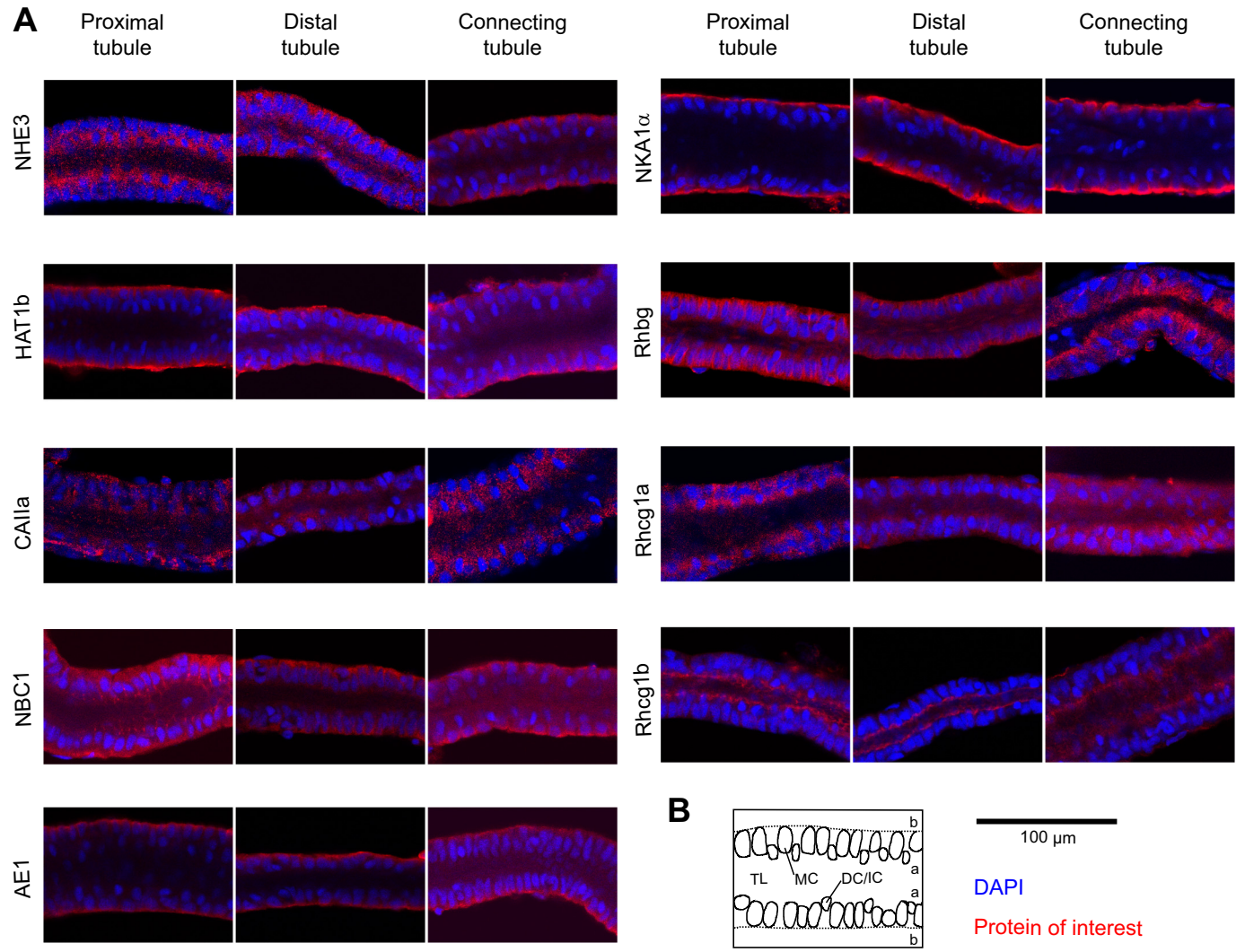

Fig. 8. Localization of proteins of interests (POI) along the kidney tubule of fed goldfish. Immunohistochemical detection of proteins in whole-mounted proximal, distal, and connecting tubules of *Carassius auratus* kidney 3 h after feeding. *A*: antibodies for Na^+/H^+-exchanger isoform 3 (NHE3), V-H^+-ATPase subunit 1b (HAT1b), carbonic anhydrase isoform IIa (CAIIa), Na^+/HCO_3^--cotransporter isoform 1 (NBC1), anion exchanger 1 (AE1), Na^+/K^+-ATPase α-subunit (NKA1α), Rhesus protein isoform bg (Rhbg), Rhesus protein isoform cg1a (Rhcg1a), and Rhesus protein isoform cg1b (Rhc1b), as described in Table 2. Cell nuclei were stained with DAPI (blue) and POIs with Alexa Fluor-546 (red). *B*: schematic drawing of points of interest after Sakai (62). a, apical; b, basal; DC, dark cell (in proximal and distal tubule); IC, interjacent cell (in connecting tubule); MC, main cell; TL, tubule lumen.

animals compared with fasted goldfish, while in DT, it appeared to be more apical. Surprisingly, Rhbg protein of fed *C. auratus* appeared to be localized in the apical membrane of CT rather than basolaterally.

Although not all four cell types as described by Sakai (62) could be distinguished in the fluorescent IHC, a distinction between main cells and the interposed, apically situated dark (PT and DT) or interjacent cells (CT) was prominent (Figs. 7*B* and 8*B*). Protein expression of all investigated genes seemed to be restricted to the main cells.

Overall, semiquantification of protein expression using average fluorescence per cell (Fig. 9) showed a much more homogenous expression of all transporters in the investigated sections PT, DT, and CT of fasted goldfish compared with the respective mRNA expression patterns. Even in the PT of fasted goldfish, NHE3 (Fig. 9*A*), NBC1 (Fig. 9*D*), NKA1α (Fig. 9*F*), Rhcg1a (Fig. 9*H*), and Rhcg1b (Fig. 9*I*) protein was clearly present, contrasting to findings in mRNA levels. The DT of fasted animals seemed to have higher expression levels for all transporters compared with the PT and also compared with the CT, except for the three Rhesus proteins. Protein expression for Rhcg1b even decreased consistently from PT to DT to CT in fasted *C. auratus*.

Comparison of protein expression in tubule sections from fasted vs. fed goldfish showed a significant upregulation of NHE3 protein in PT of fed goldfish, as well as a tendency for upregulation in DT ($P = 0.09$, Fig. 9*A*). HAT1b was statistically unchanged but showed a downward trend in CT of fed animals ($P = 0.07$, Fig. 9*B*). CAIIa protein was significantly upregulated only in DT of fed *C. auratus* (Fig. 9*C*), a pattern that was also observed for Rhcg1a (Fig. 9*H*). While NBC1 (Fig. 9*D*) and NKA1α (Fig. 9*F*) protein expression did not change in response to feeding, AE1 showed the strongest response and this protein was downregulated in all three investigated sections PT, DT, and CT (Fig. 9*E*). Rhbg (Fig. 9*G*) protein expression decreased significantly only in the DT

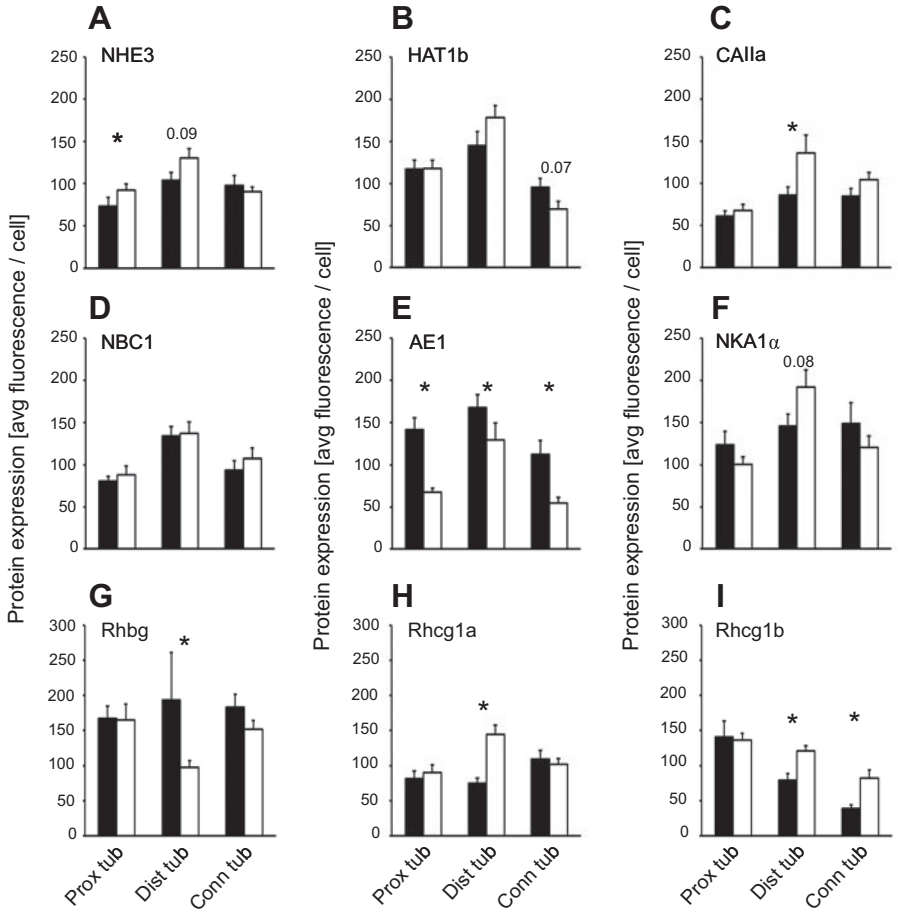

Fig. 9. Profile of protein expression, as quantified by fluorescence intensity, of epithelial transporters relevant for acid-base and ammonia balance in the different kidney tubule sections, and their responses to feeding. *A*: Na^+/H^+-exchanger isoform 3. *B*: V-H^+-ATPase subunit 1b. *C*: carbonic anhydrase isoform IIa. *D*: Na^+/HCO_3^--cotransporter isoform 1. *E*: anion exchanger 1. *F*: Na^+/K^+-ATPase α-subunit. *G*: Rhesus protein isoform bg. *H*: Rhesus protein isoform cg1a. *I*: Rhesus protein isoform cg1b. *Significant differences between fasted (96 h; black bars) and fed (3 h after feeding; open bars) goldfish (Student's *t*-test, $P < 0.05$). Values are expressed as means ± SE; $n = 3–8$.

of fed goldfish, whereas Rhcg1b (Fig. 9*I*) protein expression increased in DT and CT of fed animals.

DISCUSSION

Overview

The present study builds upon the work of Sakai (62) and links expression profiles for various renal genes and proteins to the general morphology of the goldfish kidney and renal tubules. By microdissecting isolated intact nephrons, we were able to characterize the spatial profiles of mRNA and protein expression for various epithelial transporters.

In support of our first hypothesis, expression of ion, acid-base, and ammonia transporters varied considerably among different segments of the nephron and showed many parallels to the mammalian kidney, as will be discussed below. Our results are, however, only partially supportive of the model for renal acid-base regulation in the goldfish kidney, as introduced by Lawrence et al. (39) in Fig. 7 of their paper. In contrast to their interpretation of their data, we clearly show a basolateral distribution of the V-H^+-ATPase and an additional expression of Rhcg1a in the basolateral membrane and/or the cytoplasm. However, our data do support their statement that renal ammonia excretion and acid-base regulation does not solely depend on Na^+/NH_4^+ exchange (via NHE), and does involve the intracellular process of ammoniagenesis.

In support of our second hypothesis, we provide the first molecular evidence that the expression of the investigated transporters changes following feeding, in accord with typical responses to metabolic acidosis seen in the mammalian nephron. Our data also indicate that the proximal tubule is the major site for ammoniagenesis and that the urinary bladder and Wolffian ducts express many of the transporters seen in the various parts of the nephron, therefore likely playing roles in the response to feeding and in the final polishing of the urine.

Functional Morphology

By deconstructing the goldfish kidney, we were able to verify the overall morphological traits described in Sakai's (62) study on Araldite502- or paraffin-embedded whole kidney sections. Of particular note, there was a morphological distinction between the narrow distal tubule (DT) and the wider collecting tubule (CT), which has not been mentioned in some previous studies, e.g., Chasiotis and Kelly (15). A difference in mRNA levels between the two sections was also observed for most of the investigated epithelial transporters. Indeed, with respect to mRNA levels, the CT seemed to resemble the morphologically different (i.e., even wider) collecting duct (CD). Thus, the CT might represent a transition zone with the latter section.

Although the overall organization of the goldfish kidney seemed more unstructured than the clear zonation into cortex and medulla observed in the mammalian kidney, our dissection indicated nonrandom association of glomeruli with other parts

of the tubules. Especially after the area where the proximal tubule (PT) leads into the DT, glomeruli from either the same tubule or other tubules were firmly attached to this part by connective tissue (Fig. 3, *D* and *E*). This indicates the potential for a structure comparable to the juxtaglomerular apparatus in the mammalian kidney, providing a feedback loop that would enable the adjustment of urine flow with regard to the resulting excretion of NaCl (3). Additionally, the late DT and CT exhibited a tight association and were engulfed in connective tissue, making it difficult to tease them apart (Fig. 3*F*). This tight association might also provide a feedback and/or countercurrent mechanism for the fine adjustment of the urine.

Role of the Kidney in Response to Feeding

Agastric (stomachless) freshwater fishes like the killifish, *Fundulus heteroclitus*, experience an "acidic tide" upon feeding, indicated by a drop of blood pH and [HCO_3^-] while maintaining an alkaline intestine (81). The increase in urine inorganic phosphate as an indicator for increased protons (titratable acid), the associated drop in urine pH at 3 h, and the rise in urine total ammonia at 6 h after feeding (Fig. 2) all indicate that an acidic tide (i.e., metabolic acid load) also likely occurs in the agastric goldfish, *C. auratus*. It is notable that whole animal ammonia excretion peaked at 2–4 h after feeding (Fig. 1), in contrast to the urinary ammonia peak at 6 h (Fig. 2*A*). The bulk of the feeding-induced ammonia load was likely rapidly cleared by the gills, while the delayed urinary ammonia peak probably reflected increased provision of ammonia by ammoniagenesis so as to serve as a urinary buffer (39). In general, all of these responses to feeding in the goldfish were resolved more quickly than the responses accompanying the postfeeding alkaline tide in the gastric rainbow trout (8, 9, 18, 80). In the trout, the contribution of the kidney was small relative to that of the gills in correcting the postfeeding acid-base disturbance; this remains to be quantified in the goldfish.

mRNA Expression in the Whole Kidney vs. Renal Tubule Sections

To date, changes in renal mRNA expression levels upon a disturbance of acid-base and/or ammonia equilibrium in freshwater fishes have been investigated only at the whole kidney level [i.e., goldfish (39) and common carp (86)]. Both of these studies reported an increase in mRNA expression of ammonia transport proteins upon a metabolic acidosis caused by exposure to low environmental pH (pH 4.0). However, while Lawrence et al. (39) observed upregulation of Rhcg1b (Rhcg2, Rhcg-b), Wright et al. (86) found upregulation of Rhcg1a (Rhcg1, Rhcga). Additionally, NHE3, HAT, and Na^+/K^+-ATPase (NKA) mRNA were upregulated in common carp (86), while HAT1b was slightly downregulated in goldfish (39). In the present study, NHE3 and Rhcg1b (Rhcg2, Rhcgb) mRNA and protein levels were also upregulated in response to feeding, supporting the involvement of these transporters in renal acid-base and ammonia regulation. While the same direction of overall change of NHE3 and Rhcg1b (Rhcg2, Rhcgb) could be verified by looking at the specific sections, whole kidney analysis could not provide a clear picture of when transporters exhibited a mixed response in different kidney tubule sections. For example, mRNA levels for carbonic anhydrase II (CAIIa) were upregulated in DT and downregulated in CT and CD (Fig. 5*C*), while Rhbg showed the opposite response (Fig. 5*G*), but both genes showed no change at the whole kidney level (Fig. 4*A*). Hence, the present study demonstrates that looking at whole kidney, mRNA levels will lead to an underestimation of the actual changes that are occurring. Reassuringly, however, the majority of changes observed at the mRNA level translated into changes in protein expression.

Indications for Ammoniagenesis

In mammals, the major source of urinary ammonia is renal production (ammoniagenesis via glutamine) rather than glomerular filtration (74). The PT plays a major role in ammoniagenesis in response to a metabolic acidosis, although there is evidence that generally, most renal sections are capable of ammoniagenesis (24). In the goldfish, two of the major enzymes involved in ammoniagenesis and the reversed reaction, GDH and GS, respectively, exhibited highest mRNA expression in the PT (Fig. 6). Although GDH is involved in the breaking down of glutamate to NH_4^+ and HCO_3^-, GS uses NH_4^+ to regenerate glutamine and, therefore, decreases net NH_4^+ formation (74). Indeed, the section-specific mRNA expression pattern of these enzymes observed in the present study, as well as the responses to feeding, corresponded well with the profile observed in mammals (74). Thus, GS protein expression is highest in the PT of rats and rabbits (11), and its activity, as well as expression, significantly decreased in response to a metabolic acidosis in mice (16), while the activity and expression of GDH protein significantly increased (68, 74). In the goldfish, both whole kidney and section-specific responses to feeding were qualitatively similar to those reported to metabolic acidosis in mammals, with an increase in GDH expression and a decrease in GS expression, particularly in the PT (Fig. 6). Unfortunately, replicate numbers were low for the early tubule sections where expression levels were highest, but the consistent results for the remaining tubule sections compared with the mammalian kidney, together with the supporting results for the whole goldfish kidney (Fig. 4*B*), make a convincing case for an increase of ammoniagenesis in response to feeding.

Expression of Epithelial Transporters under Fasting Conditions Along the Tubule Sections

In the mammalian kidney, distinct renal tubule sections fulfill different purposes (32), and there appear to be considerable parallels in the goldfish kidney.

Proximal tubule. Interestingly, in the kidney of fasted goldfish, hardly any expression of mRNA for NHE3, NBC1, NKA1α, Rhcg1a, and Rhcg1b could be detected in the PT (Fig. 5). When looking at protein expression, however, all transporters were clearly present in this section (Figs. 7 and 9). This might indicate high turnover rates for the transporters' mRNA into protein, probably due to a high activity of the tissue (i.e., ammoniagenesis, as described above).

In mammals, apical ammonia transport in this major site of ammoniagenesis (24) seems to be mainly mediated by NHE3 working in conjunction with HAT. Surprisingly, however, NHE3 and HAT were restricted to the basal/basolateral membrane in the PT of fasted goldfish. In fishes, even though HAT was identified apically in an undefined subpopulation of kidney

tubule cells in rainbow trout (53), basal and/or basolateral HAT was observed in the interlamellar filament epithelium of glass eel gills (78), and the mitochondria-rich cells of gills of killifish (34) and stingray (56), analogous to the base-secreting B-type mitochondria-rich intercalated cell of the vertebrate kidney (6). Furthermore, in both seawater and freshwater trout, HAT was colocalized with basolateral NKA and AE1 in the PT (35). Distribution of HAT (7) and NHE3 (61) is believed to be highly dependent on vesicle trafficking and the microtubule network. When disrupted by colchicine, NHE3 protein was identified in the basolateral rather than in the apical membrane of PT in rats (61). In gills of fed dogfish, which have an acid-secreting stomach, HAT was relocalized to the basolateral membrane to counteract the alkaline tide experienced after feeding (69). In the present scenario of the goldfish, a basolateral localization of NHE3 (and HAT) might simply indicate that under fasted conditions, an apical proton secretion is not needed; indeed, a basolateral proton export is in accord with the normally alkaline urine produced by fasting goldfish (Fig. 2 (39). This changes during an acid-load generated by feeding, as indicated by the relocalization of NHE3 to the apical membrane as observed in the present study.

Furthermore, in mammals, a basolateral electrogenic 1 Na^+/HCO_3^--cotransporter (NBCe1) in the PT leads to the reabsorption of Na^+ and HCO_3^-, respectively (76). This protein was also identified in the basolateral membrane in *C. auratus*, as was basolateral AE1. Consequently, it can be hypothesized that the PT in goldfish is mainly involved in the reabsorption of Na^+ (NBCe1) and Cl^- (AE1), and base in the form of HCO_3^- (NBCe1), energized by a basal NKA. Again, this could contribute to the alkalinity of the urine under fasting conditions (39).

Additionally, all three Rhesus proteins Rhbg, Rhcg1a, and Rhcg1b are present in this section, indicating a potential for apical secretion of ammonia via Rhcg1a and/or Rhcg1b, and/or basal reabsorption of ammonia via Rhbg. There have been intensive discussions about whether Rhesus proteins transport the gaseous (NH_3) or ionic (NH_4^+) forms of ammonia (2). Given that intracellular pH under control conditions is generally lower than plasma and environmental pH (14), and ammoniagenesis takes place in epithelial cells, the gradient of NH_4^+ would support basolateral and apical exit of NH_4^+ out of the cell either into the plasma (via basolateral Rhbg and/or Rhcg1a) or the environment (via apical Rhcg1a and/or Rhcg1b), respectively. Furthermore, Rhcg in mammals is also expressed in vesicles in the cytoplasm (64), creating a pool that could be translocated into the apical or basolateral membrane as needed. IHC data of the present study in goldfish renal tubules indicate, indeed, that Rhcg1a protein might serve as the intracellular pool, while Rhcg1b and Rhbg proteins would provide the constant pathways for ammonia to exit the cell apically (secretion) or basolaterally (reabsorption), respectively.

Distal tubule. Some ammonia secretion takes place in the distal section in rats, and it increases upon a metabolic acidosis (65). The exact mechanisms, however, are not fully understood to date (76). Immunohistochemical studies verified the expression of both basolateral Rhbg, as well as apical and basolateral Rhcg in DT of rats, although at a lower level compared with the connecting segment and collecting duct (CD) (57). All three Rhesus proteins (basolateral Rhbg, basolateral, and/or apical and/or cytoplasmic Rhcg1a and apical Rhcg1b) were also expressed in goldfish DTs (Figs. 7 and 9). While Rhbg additionally exhibited the second largest expression of all investigated mRNAs, Rhcg1a and Rhcg1b mRNAs were hardly detectable. This indicates a more important role for Rhbg in the sense that it can be translated quickly when needed. With a basolateral NHE3 and HAT, the DT section seems to be generally more involved in the reabsorption of Na^+ (NHE3) and ammonia (via Rhbg potentially facilitated by basolateral protons by HAT), as observed in mammals.

Connecting tubule and collecting duct. The suite of transporters in the mammalian connecting segment resembles closely those observed in the CD (76), including the presence of Rhbg and Rhcg (72). The mammalian CD seems to be responsible for the majority of ammonia secretion (74, 76). The process is complex and includes the actions of apical Rhcg and HAT, basolateral Rhbg and potentially Rhcg, NKA and AE1, as well as cytoplasmic CA (CAII).

Unfortunately, although we were able to obtain protein expression data for the CT of the goldfish kidney, we were unable to investigate the CD due to limitations of the whole-mount technique. The CT, however, expressed all of the above proteins, and CT and CD had similar mRNA expression patterns for all investigated transporters (Figs. 5 and 9), suggesting that similar mechanisms are present in these two sections. As in mammals, this indicates that there may be no real distinction in function between these sections.

Compared with other sections, goldfish CT and CD exhibited high levels of mRNA for NHE3 (highest overall expression level of any transporter), CAIIa and Rhcg1a (Fig. 5). This might indicate these to be major sites for immediate adjustments to acid-base and/or ammonia disturbances, as proteins could be quickly translated as needed. These three genes, NHE3, CAIIa, and Rhcg1a, might form a functional unit as has been shown for the mammalian CD (75). Supporting a potential colocalization of NHE3b and Rhcg1a in a teleost tissue are the studies of the yolk-sac epithelium of developing rainbow trout, as well as PNA^+ cells of the ionocytes of adult rainbow trout gills (88). Interestingly, however, although in trout gills and yolk sacs, as well as mammals, this complex promotes the apical secretion of protons and ammonia, in goldfish, it might rather help in the reabsorption of these components, especially under fasting conditions, as IHC showed a potential basolateral expression of the NHE3 protein as well as Rhcg1a. Consequently, in contrast to mammals, ammonia secretion in the goldfish under fasting conditions may be attributed to a larger extent to the DT compared with the CT/CD.

Wolffian duct. mRNAs of Rhcg1a and Rhcg1b, NKA1α, HAT1b, and AE1 were expressed in the Wolffian duct (both in kidney and body) at moderate levels (Fig. 5), indicating potential roles in both H^+ and ammonia adjustments in this kidney section. Strikingly, mRNA expression for NBC1 is much higher in this section compared with the earlier sections in fasting goldfish. NBC1 has, therefore, a unique expression pattern compared with all other transcripts and potentially promotes basolateral exit of HCO_3^- in this later tubule section in accord with the alkaline urine of fasting goldfish (39). This

is similar to the situation in the mammalian PT (27, 76). However, other NBC isoforms could be present in the goldfish. In mammals, for example, the electroneutral basolateral transport of HCO_3^- into the cells of the thick ascending limb of the Loop of Henle is promoted by NBCn1 (40, 76). Further investigation is needed of the roles of potentially different NBCs in the teleost kidney.

Expression Responses of Epithelial Transporters in Different Tubule Sections upon Feeding

General observations. HAT1b and AE1 were the only transcripts to have a homogenous, overall moderate mRNA expression level that stayed more or less constant with feeding in all investigated tubule sections (Fig. 5). AE1 protein expression in contrast to HAT protein, however, showed a pronounced downregulation in PT, DT, and CT (Fig. 9). NBC1 on the other hand, even though exhibiting a more alternating mRNA expression pattern in different tubule sections, was constant in mRNA and protein expression from PT to CT, as well as between fasted and fed animals. Hence, we postulate that HAT ensures a general baseline level of transport with regard to H^+ throughout all kidney sections, and NBC1 with regard to HCO_3^- in the earlier tubule sections. Because of the lack of a pronounced response upon feeding in both mRNA and protein expression, a similar "housekeeping" role might be the case for NKA as the major electrogenic driver for ion transport.

In contrast, NHE3, CAIIa, and AE1, as well as the ammonia channels Rhbg and Rhcg1b, exhibited substantial changes in response to feeding in distinct tubule sections in both mRNA (Fig. 5) and protein expression (Fig. 9). While mRNA expression levels of Rhcg1a did not respond to feeding, we observed a significant upregulation of Rhcg1a protein in the DT.

We also observed similar responses for the mRNA expression of enzymes involved in ammoniagenesis as in mammals (see above), as well as differential regulation of mRNA expression of transporters in specific tubule sections.

Comparison of section-specific responses to feeding in goldfish to renal responses to a metabolic acidosis in mammals. Strikingly, AE1 protein expression was the most affected of all investigated transporters (Fig. 9*E*), even though it did not exhibit a pronounced response at the mRNA level (Fig. 5*E*) to the metabolic acidosis caused by feeding. The observed decrease in basolateral AE1 throughout the PT, DT, and CT after feeding would help decrease the high HCO_3^- content of the urine, which is typical of the fasting condition in the goldfish (39), thereby retaining HCO_3^- in the plasma to buffer and elevate blood pH in the face of the acidosis. In rats, a metabolic acidosis resulted in the upregulation of basolateral AE1 in the A-type intercalated cells of the CD (60). It has to be noted, however, that in mammals, a basolateral AE is believed to relocate HCO_3^- into the plasma, while taking Cl^- up into the cell, a process that is likely inverted in a freshwater teleost to prevent Cl^- loss and produce a urine high in [HCO_3^-] under fasting conditions. Hence, in these two different physiological scenarios, the opposite response of AE1 would be expected.

In response to a metabolic acidosis, the importance of NHE3 in promoting the increase in ammonia excretion in the PT has been verified in rats, although this was mediated at the protein activity rather than the mRNA level (1), in response to endothelin-1/endothelin-B (38), or ANG II (49). In goldfish, we see a significant increase in both mRNA (Fig. 5*A*), as well as protein expression levels for NHE3 (Fig. 9*A*). Interestingly, the PT was the only renal tubule section with an apical localization for this transporter under fed conditions. Hence, we postulate a very similar NHE3-mediated increase in ammonia secretion in the goldfish as seen in mammals. At the very least, it suggests an overall increased acid-excretion capacity in response to feeding and underlines the role of the kidney in acid-base balance.

To date, the processes in the mammalian DT and its responses to an metabolic acidosis are incompletely understood (76). In the goldfish DT, CAIIa, Rhcg1a, and Rhcg1b mRNA levels were upregulated by feeding (Fig. 5) despite their already high expression level under fasted conditions, which was consistent with protein expression levels (Fig. 9). Even though not significant, a trend for upregulation was also observed in NHE3 protein (here basolateral), while upregulation of NHE3 at the mRNA level was very marked.

Interestingly, mRNA and protein expression for the cytosolic isoform of CA in the kidney of rainbow trout, tCAc (here CAII), was upregulated in response to a respiratory acidosis caused by hypercapnia (23). In contrast to the membrane-bound isoform, which was only present in the PT and did not respond to the stressor, tCAc was identified in apical and basolateral regions of both PT and DT (23). Our results for the cytosolic isoform are consistent with these findings and support the importance of a cytosolic carbonic anhydrase in renal acid-base regulation in fishes.

Additionally, on the basis of the goldfish data in the present study, it seems that the DT increases ammonia secretion upon feeding as a response to the increase in ammoniagenesis, as discussed above. This could be accomplished via increased apical Rhcg1b and potentially Rhcg1a, while at the same time decreasing basolateral Rhbg and, therefore, ammonia reabsorption. Interestingly, a similar response to a metabolic acidosis was observed in rat renal intercalated cells of the CD: total and apical plasma membrane Rhcg expression was increased while intracellular Rhcg expression decreased (64). Hence, our results provide some insight into potential processes that might also be applicable in mammals.

In the mammalian CD, the enhanced apical ammonia secretion in response to a metabolic acidosis seems to be promoted mainly by an increase in apical Rhcg protein expression (64). An important role for Rhcg in multiple nephron segments was also observed in mice that were fed a high-protein/high-sulfur amino acid-enriched diet (5). Accordingly, in the present study, we observed a marked upregulation of Rhcg1b mRNA and protein in response to the acid- and ammonia-load caused by feeding. As in mammals, there may be no real distinction in function between the CD and the CT. Upregulation of Rhbg mRNA, Rhcg1b mRNA, and protein, and downregulation of CAIIa mRNA expression in response to feeding, were similar in the two sections in goldfish (Figs. 5 and 9). Interestingly, while barely detectable under fasting conditions, the overall mRNA expression pattern for Rhcg1b in response to feeding became very similar to the overall expression pattern of Rhcg1a. We postulate that apical Rhcg1a could ensure baseline ammonia secretion, because mRNA and protein levels were hardly affected by feeding but highly expressed in CT and CD (Figs. 5*H* and 9*H*). Rhcg1b on the other hand, with generally

lower expression at both mRNA and protein levels (Figs. 5*I* and 9*I*), would change to meet the acid-base challenge and, hence, the observed upregulation of Rhcg1b protein, but not Rhcg1a, in CT in response to feeding. In the CD, also Rhbg mRNA expression was significantly upregulated in goldfish, as it was similarly observed in the cortex and medulla of mice (4). Surprisingly, however, Rhbg protein in goldfish seemed to switch from its typical and expected basolateral expression under fasted conditions (Fig. 7) to an apical localization in fed animals (Fig. 8). This might serve to even further increase ammonia secretion in this section.

Hardly any changes in mRNA expression upon feeding were observed in the Wolffian duct, suggesting a negligible role for adjustments of the urine in this section, similar to what has been proposed for the mammalian ureter [<10% change of urea and solutes (73)]. The upregulation of Rhbg and downregulation of Rhcg1a in concert with changes in ammoniagenesis-relevant genes (Figs. 5 and 6), however, might indicate a potential role for this section in renal ammonia metabolism and ammonia reabsorption in the goldfish.

Overall, the section-specific responses observed in goldfish in response to feeding clearly paralleled many aspects of the mammalian response to a metabolic acidosis, in support of our second hypothesis.

Potential Role of the Bladder in Response to Feeding and in Fine-Tuning the Urine

In mammals, the bladder is a muscular organ, but its epithelium (urothelium) possesses many tight junctions and exhibits a very low permeability for ions and, hence, can be regarded as a barrier to maintain urine composition similar to that delivered by the kidney (41). The urothelium, however, does exhibit some capacity for active Na^+ transport, as passive diffusion of Na^+ from the extracellular space into the lumen is counteracted by amiloride-sensitive active apical Na^+ transport in rabbits (42). Furthermore, the basolateral epithelium seems to contain potassium and chloride channels, Na^+/H^+ exchangers, as well as Cl^-/HCO_3^- exchangers (41). In teleost fishes, the bladder is a thin, nonmuscular organ formed by the fusion of the Wolffian (archinephric) ducts (28). Most in vivo studies investigating renal function of teleost fishes have used internal bladder catheterization, thereby negating storage of urine that would allow for its composition to be modified by epithelial transport processes (e.g., 28, 39, 79). However, Curtis and Wood (19), using a urine collection technique that allowed the bladder to function normally, reported that in rainbow trout, significant reabsorption of Na^+ and Cl^-, and possible reabsorption of ammonia and K^+, took place in the 25-min period that urine is naturally stored in this organ before being periodically released into the environment. This was in accord with other in vitro studies showing active reabsorption of Na^+ and Cl^- across this organ in trout (12, 22, 44), indicating the capacity for a targeted fine-tuning of the urine composition.

In the present study, mRNA expression of HAT1b, CAIIa, NBC1, AE1, and NKA1α could be detected under fasted conditions in the bladder (Fig. 5), in accord with the capacity for active adjustment (fine-tuning) of urine ionic composition. Interestingly, NBC1 had a unique expression pattern with very low mRNA levels in the early tubule sections, but had the highest mRNA expression in the Wolffian duct and bladder. Feeding resulted in significant upregulation of NHE3 and Rhcg1b, as well as a marked downregulation of NBC1 (Fig. 5). As in mammals and trout (see above), these results indicate the potential for active ionic regulation by the bladder. Apical reabsorption of Na^+ by NHE3 may facilitate the simultaneous secretion of ammonia via Rhcg1b by H^+ trapping after feeding. There might, however, at the same time be a decreased basolateral reabsorption of Na^+ (and HCO_3^-) via NBC1, as the mRNA expression levels of this transporter decreased by 90%. Clearly, future experiments are needed to further elucidate the potential active epithelial transport capacity of the bladder epithelium in teleost fishes.

ACKNOWLEDGMENTS

We thank Dr. Denis Lynn [Department of Zoology, University of British Columbia (UBC)] for lending us his microscope for the dissections, Patrick Tamkee, and Eric Lotto for help in the aquatics facility, and Garnet Martens and Kevin Hodgson (Bioimaging Facility at UBC) for help with the confocal work. We also thank Drs. Dirk Weihrauch and W. Gary Anderson (University of Manitoba) for providing space and equipment for the Western blot analysis, and everyone listed in Table 2 for providing the antibodies.

GRANTS

This work was funded by a Natural Sciences and Engineering Research Council Discovery grant to C. M. Wood.

DISCLOSURES

No conflicts of interest, financial or otherwise, are declared by the authors.

AUTHOR CONTRIBUTIONS

S.F. performed experiments; S.F. analyzed data; S.F. interpreted results of experiments; S.F. prepared figures; S.F. drafted manuscript; S.F. and C.M.W. edited and revised manuscript; S.F. and C.M.W. approved final version of manuscript.

REFERENCES

1. **Ambühl PM, Amemiya M, Danczkay M, Lötscher M, Kaissling B, Moe OW, Preisig PA, Alpern RJ.** Chronic metabolic acidosis increases NHE3 protein abundance in rat kidney. *Am J Physiol Renal Physiol* 271: F917–F925, 1996. doi:10.1152/ajprenal.1996.271.4.F917.
2. **Baday S, Orabi EA, Wang S, Lamoureux G, Bernèche S.** Mechanism of NH_4^+ recruitment and NH3 transport in Rh proteins. *Structure* 23: 1550–1557, 2015. doi:10.1016/j.str.2015.06.010.
3. **Barajas L.** Anatomy of the juxtaglomerular apparatus. *Am J Physiol Renal Physiol* 237: F333–F343, 1979. doi:10.1152/ajprenal.1979.237.5.F333.
4. **Bishop JM, Verlander JW, Lee H-W, Nelson RD, Weiner AJ, Handlogten ME, Weiner ID.** Role of the Rhesus glycoprotein, Rh B glycoprotein, in renal ammonia excretion. *Am J Physiol Renal Physiol* 299: F1065–F1077, 2010. doi:10.1152/ajprenal.00277.2010.
5. **Bounoure L, Ruffoni D, Müller R, Kuhn GA, Bourgeois S, Devuyst O, Wagner CA.** The role of the renal ammonia transporter Rhcg in metabolic responses to dietary protein. *J Am Soc Nephrol* 25: 2040–2052, 2014. doi:10.1681/ASN.2013050466.
6. **Brown D, Breton S.** H^+V-ATPase-dependent luminal acidification in the kidney collecting duct and the epididymis/vas deferens: vesicle recycling and transcytotic pathways. *J Exp Biol* 203: 137–145, 2000.
7. **Brown D, Sabolic I, Gluck S.** Colchicine-induced redistribution of proton pumps in kidney epithelial cells. *Kidney Int Suppl* 33: S79–S83, 1991.
8. **Bucking C, Landman MJ, Wood CM.** The role of the kidney in compensating the alkaline tide, electrolyte load, and fluid balance disturbance associated with feeding in the freshwater rainbow trout, *Oncorhynchus mykiss*. *Comp Biochem Physiol A Mol Integr Physiol* 156: 74–83, 2010. doi:10.1016/j.cbpa.2009.12.021.
9. **Bucking C, Wood CM.** The alkaline tide and ammonia excretion after voluntary feeding in freshwater rainbow trout. *J Exp Biol* 211: 2533–2541, 2008. doi:10.1242/jeb.015610.

10. **Bucking C, Wood CM.** Digestion of a single meal affects gene expression of ion and ammonia transporters and glutamine synthetase activity in the gastrointestinal tract of freshwater rainbow trout. *J Comp Physiol B* 182: 341–350, 2012. doi:10.1007/s00360-011-0622-y.
11. **Burch HB, Choi S, McCarthy WZ, Wong PY, Lowry OH.** The location of glutamine synthetase within the rat and rabbit nephron. *Biochem Biophys Res Commun* 82: 498–505, 1978. doi:10.1016/0006-291X(78)90902-6.
12. **Burgess DW, Miarczynski MD, O'Donnell MJ, Wood CM.** Na^+ and Cl^- transport by the urinary bladder of the freshwater rainbow trout (*Oncorhynchus mykiss*). *J Exp Zool* 287: 1–14, 2000. doi:10.1002/1097-010X(20000615)287:1<1::AID-JEZ1>3.0.CO;2-4.
13. **Cameron JN, Kormanik GA.** The acid-base responses of gills and kidneys to infused acid and base loads in the channel catfish, *Ictalurus punctatus*. *J Exp Biol* 99: 143–160, 1982.
14. **Casey JR, Grinstein S, Orlowski J.** Sensors and regulators of intracellular pH. *Nat Rev Mol Cell Biol* 11: 50–61, 2010. doi:10.1038/nrm2820.
15. **Chasiotis H, Kelly SP.** Occludin immunolocalization and protein expression in goldfish. *J Exp Biol* 211: 1524–1534, 2008. doi:10.1242/jeb.014894.
16. **Conjard A, Komaty O, Delage H, Boghossian M, Martin M, Ferrier B, Baverel G.** Inhibition of glutamine synthetase in the mouse kidney: a novel mechanism of adaptation to metabolic acidosis. *J Biol Chem* 278: 38159–38166, 2003. doi:10.1074/jbc.M302885200.
17. **Cooper CA, Wilson JM, Wright PA.** Marine, freshwater and aerially acclimated mangrove rivulus (*Kryptolebias marmoratus*) use different strategies for cutaneous ammonia excretion. *Am J Physiol Regul Integr Comp Physiol* 304: R599–R612, 2013. doi:10.1152/ajpregu.00228.2012.
18. **Cooper CA, Wilson RW.** Post-prandial alkaline tide in freshwater rainbow trout: effects of meal anticipation on recovery from acid-base and ion regulatory disturbances. *J Exp Biol* 211: 2542–2550, 2008. doi:10.1242/jeb.015586.
19. **Curtis BJ, Wood CM.** The function of the urinary bladder in vivo in the freshwater rainbow trout. *J Exp Biol* 155: 567–583, 1991. doi:10.1002/jez.10080.
20. **Curtis BJ, Wood CM.** Kidney and urinary bladder responses of freshwater rainbow trout to isosmotic NaCl and $NaHCO_3$ infusion. *J Exp Biol* 173: 181–203, 1992.
21. **Dantzler WH.** *Comparative Physiology of the Vertebrate Kidney* (2nd ed.). New York: Springer Science+Business Media, 2016.
22. **Fossat B, Lahlou B.** Osmotic and urinary permeabilities of isolated urinary bladder of the trout. *Am J Physiol Renal Physiol* 233: F525–F531, 1977. doi:10.1152/ajprenal.1977.233.6.F525.
23. **Georgalis T, Gilmour KM, Yorston J, Perry SF.** Roles of cytosolic and membrane-bound carbonic anhydrase in renal control of acid-base balance in rainbow trout, *Oncorhynchus mykiss*. *Am J Physiol Renal Physiol* 291: F407–F421, 2006. doi:10.1152/ajprenal.00328.2005.
24. **Good DW, Burg MB.** Ammonia production by individual segments of the rat nephron. *J Clin Invest* 73: 602–610, 1984. doi:10.1172/JCI111250.
25. **Hamm LL, Nakhoul N, Hering-Smith KS.** Acid-base homeostasis. *Clin J Am Soc Nephrol* 10: 2232–2242, 2015. doi:10.2215/CJN.07400715.
26. **Hammer Ø, Harper DAT, Ryan PD.** PAST: Paleontological statistics software package for education and data analysis. *Palaeontol Electronica* 4: 1–9, 2001.
27. **Handlogten ME, Osis G, Lee H-W, Romero MF, Verlander JW, Weiner ID.** NBCe1 expression is required for normal renal ammonia metabolism. *Am J Physiol Renal Physiol* 309: F658–F666, 2015. doi:10.1152/ajprenal.00219.2015.
28. **Hickman CP, Trump BF.** The kidney, in *Fish Physiology*, edited by Hoar WS, Randall DJ. New York: Academic Press, 1969, p. 91–239.
29. **Hoar WS, Hickman CP.** *A Laboratory Companion for General and Comparative Physiology* (2nd ed.). Upper Saddle River: Prentice Hall, 1975.
30. **Ivanis G, Braun M, Perry SF.** Renal expression and localization of SLC9A3 sodium/hydrogen exchanger and its possible role in acid-base regulation in freshwater rainbow trout (*Oncorhynchus mykiss*). *Am J Physiol Regul Integr Comp Physiol* 295: R971–R978, 2008. doi:10.1152/ajpregu.90328.2008.
31. **Ivanis G, Esbaugh AJ, Perry SF.** Branchial expression and localization of SLC9A2 and SLC9A3 sodium/hydrogen exchangers and their possible role in acid-base regulation in freshwater rainbow trout (*Oncorhynchus mykiss*). *J Exp Biol* 211: 2467–2477, 2008. doi:10.1242/jeb.017491.
32. **Jacobson HR.** Functional segmentation of the mammalian nephron. *Am J Physiol Renal Physiol* 241: F203–F218, 1981. doi:10.1152/ajprenal.1981.241.3.F203.
33. **Kato A, Muro T, Kimura Y, Li S, Islam Z, Ogoshi M, Doi H, Hirose S.** Differential expression of Na^+-Cl^- cotransporter and Na^+-K^+-Cl^- cotransporter 2 in the distal nephrons of euryhaline and seawater pufferfishes. *Am J Physiol Regul Integr Comp Physiol* 300: R284–R297, 2011. doi:10.1152/ajpregu.00725.2009.
34. **Katoh F, Hyodo S, Kaneko T.** Vacuolar-type proton pump in the basolateral plasma membrane energizes ion uptake in branchial mitochondria-rich cells of killifish *Fundulus heteroclitus*, adapted to a low ion environment. *J Exp Biol* 206: 793–803, 2003. doi:10.1242/jeb.00159.
35. **Katoh F, Tresguerres M, Lee KM, Kaneko T, Aida K, Goss GG.** Cloning of rainbow trout SLC26A1: involvement in renal sulfate secretion. *Am J Physiol Regul Integr Comp Physiol* 290: R1468–R1478, 2006. doi:10.1152/ajpregu.00482.2005.
36. **King PA, Goldstein L.** Renal ammonia excretion and production in goldfish, *Carassius auratus*, at low environmental pH. *Am J Physiol Regul Integr Comp Physiol* 245: R590–R599, 1983. doi:10.1152/ajpregu.1983.245.4.R590.
37. **Kurita Y, Nakada T, Kato A, Doi H, Mistry AC, Chang M-H, Romero MF, Hirose S.** Identification of intestinal bicarbonate transporters involved in formation of carbonate precipitates to stimulate water absorption in marine teleost fish. *Am J Physiol Regul Integr Comp Physiol* 294: R1402–R1412, 2008. doi:10.1152/ajpregu.00759.2007.
38. **Laghmani K, Preisig PA, Moe OW, Yanagisawa M, Alpern RJ.** Endothelin-1/endothelin-B receptor-mediated increases in NHE3 activity in chronic metabolic acidosis. *J Clin Invest* 107: 1563–1569, 2001. doi:10.1172/JCI11234.
39. **Lawrence MJ, Wright PA, Wood CM.** Physiological and molecular responses of the goldfish (*Carassius auratus*) kidney to metabolic acidosis, and potential mechanisms of renal ammonia transport. *J Exp Biol* 218: 2124–2135, 2015. doi:10.1242/jeb.117689.
40. **Lee S, Lee HJ, Yang HS, Thornell IM, Bevensee MO, Choi I.** Sodium-bicarbonate cotransporter NBCn1 in the kidney medullary thick ascending limb cell line is upregulated under acidic conditions and enhances ammonium transport. *Exp Physiol* 95: 926–937, 2010. doi:10.1113/expphysiol.2010.053967.
41. **Lewis SA.** Everything you wanted to know about the bladder epithelium but were afraid to ask. *Am J Physiol Renal Physiol* 278: F867–F874, 2000. doi:10.1152/ajprenal.2000.278.6.F867.
42. **Lewis SA, Diamond JM.** Na^+ transport by rabbit urinary bladder, a tight epithelium. *J Membr Biol* 28: 1–40, 1976. doi:10.1007/BF01869689.
43. **Marini A-M, Matassi G, Raynal V, André B, Cartron J-P, Chérif-Zahar B.** The human Rhesus-associated RhAG protein and a kidney homologue promote ammonium transport in yeast. *Nat Genet* 26: 341–344, 2000. doi:10.1038/81656.
44. **Marshall WS.** Independent Na^+ and Cl^- active transport by urinary bladder epithelium of brook trout. *Am J Physiol Regul Integr Comp Physiol* 250: R227–R234, 1986. doi:10.1152/ajpregu.1986.250.2.R227.
45. **McDonald DG.** The interaction of environmental calcium and low pH on the physiology of the rainbow trout, *Salmo gairdneri*. I. Branchial and renal net ion and H^+ fluxes. *J Exp Biol* 102: 123–140, 1983.
46. **McDonald DG, Wood CM.** Branchial and renal acid and ion fluxes in the rainbow trout, *Salmo gairdneri*, at low environmental pH. *J Exp Biol* 93: 101–118, 1981.
47. **Metro-Vancouver.** *Vancouver Water Utility Annual Report—2015*. Vancouver, ON, Canada: Metro-Vancouver, 2015.
48. **Murphy J, Riley JP.** A modified single solution method for the determination of phosphate in natural waters. *Anal Chim Acta* 27: 31–36, 1962. doi:10.1016/S0003-2670(00)88444-5.
49. **Nagami GT.** Role of angiotensin II in the enhancement of ammonia production and secretion by the proximal tubule in metabolic acidosis. *Am J Physiol Renal Physiol* 294: F874–F880, 2008. doi:10.1152/ajprenal.00286.2007.
50. **Nakada T, Hoshijima K, Esaki M, Nagayoshi S, Kawakami K, Hirose S.** Localization of ammonia transporter Rhcg1 in mitochondrion-rich cells of yolk sac, gill, and kidney of zebrafish and its ionic strength-dependent expression. *Am J Physiol Regul Integr Comp Physiol* 293: R1743–R1753, 2007. doi:10.1152/ajpregu.00248.2007.
51. **Nakada T, Westhoff CM, Kato A, Hirose S.** Ammonia secretion from fish gill depends on a set of Rh glycoproteins. *FASEB J* 21: 1067–1074, 2007. doi:10.1096/fj.06-6834com.

52. **Nawata CM, Hirose S, Nakada T, Wood CM, Kato A.** Rh glycoprotein expression is modulated in pufferfish (*Takifugu rubripes*) during high environmental ammonia exposure. *J Exp Biol* 213: 3150–3160, 2010. doi:10.1242/jeb.044719.
53. **Perry SF, Fryer JN.** Proton pumps in the fish gill and kidney. *Fish Physiol Biochem* 17: 363–369, 1997. doi:10.1023/A:1007746217349.
54. **Perry SF, Gilmour KM.** Acid-base balance and CO_2 excretion in fish: unanswered questions and emerging models. *Respir Physiol Neurobiol* 154: 199–215, 2006. doi:10.1016/j.resp.2006.04.010.
55. **Perry SF, Shahsavarani A, Georgalis T, Bayaa M, Furimsky M, Thomas SLY.** Channels, pumps, and exchangers in the gill and kidney of freshwater fishes: their role in ionic and acid-base regulation. *J Exp Zoolog A Comp Exp Biol* 300: 53–62, 2003. doi:10.1002/jez.a.10309.
56. **Piermarini PM, Evans DH.** Immunochemical analysis of the vacuolar proton-ATPase B-subunit in the gills of a euryhaline stingray (*Dasyatis sabina*): effects of salinity and relation to Na^+/K^+-ATPase. *J Exp Biol* 204: 3251–3259, 2001.
57. **Quentin F, Eladari D, Cheval L, Lopez C, Goossens D, Colin Y, Cartron J-P, Paillard M, Chambrey R.** RhBG and RhCG, the putative ammonia transporters, are expressed in the same cells in the distal nephron. *J Am Soc Nephrol* 14: 545–554, 2003. doi:10.1097/01.ASN.0000050413.43662.55.
58. **Rahmatullah M, Boyde TRC.** Improvements in the determination of urea using diacetyl monoxime; methods with and without deproteinisation. *Clin Chim Acta* 107: 3–9, 1980. doi:10.1016/0009-8981(80)90407-6.
59. **Rueden CT, Schindelin J, Hiner MC, DeZonia BE, Walter AE, Arena ET, Eliceiri KW.** ImageJ2: ImageJ for the next generation of scientific image data. *BMC Bioinformatics* 18: 529, 2017. doi:10.1186/s12859-017-1934-z.
60. **Sabolić I, Brown D, Gluck SL, Alper SL.** Regulation of AE1 anion exchanger and H^+-ATPase in rat cortex by acute metabolic acidosis and alkalosis. *Kidney Int* 51: 125–137, 1997. doi:10.1038/ki.1997.16.
61. **Sabolić I, Herak-Kramberger CM, Ljubojević M, Biemesderfer D, Brown D.** NHE3 and NHERF are targeted to the basolateral membrane in proximal tubules of colchicine-treated rats. *Kidney Int* 61: 1351–1364, 2002. doi:10.1046/j.1523-1755.2002.00266.x.
62. **Sakai T.** The structure of the kidney from the freshwater teleost *Carassius auratus*. *Anat Embryol (Berl)* 171: 31–39, 1985. doi:10.1007/BF00319052.
63. **Schindelin J, Arganda-Carreras I, Frise E, Kaynig V, Longair M, Pietzsch T, Preibisch S, Rueden C, Saalfeld S, Schmid B, Tinevez J-YJ-Y, White DJ, Hartenstein V, Eliceiri K, Tomancak P, Cardona A.** Fiji: an open-source platform for biological-image analysis. *Nat Methods* 9: 676–682, 2012. doi:10.1038/nmeth.2019.
64. **Seshadri RM, Klein JD, Smith T, Sands JM, Handlogten ME, Verlander JW, Weiner ID.** Changes in subcellular distribution of the ammonia transporter, Rhcg, in response to chronic metabolic acidosis. *Am J Physiol Renal Physiol* 290: F1443–F1452, 2006. doi:10.1152/ajprenal.00459.2005.
65. **Simon E, Martin D, Buerkert J.** Contribution of individual superficial nephron segments to ammonium handling in chronic metabolic acidosis in the rat. Evidence for ammonia disequilibrium in the renal cortex. *J Clin Invest* 76: 855–864, 1985. doi:10.1172/JCI112043.
66. **Sinha AK, Liew HJ, Nawata CM, Blust R, Wood CM, De Boeck G.** Modulation of Rh glycoproteins, ammonia excretion and Na^+ fluxes in three freshwater teleosts when exposed chronically to high environmental ammonia. *J Exp Biol* 216: 2917–2930, 2013. doi:10.1242/jeb.084574.
67. **Tang CH, Lee TH.** The effect of environmental salinity on the protein expression of Na^+/K^+-ATPase, $Na^+/K^+/2Cl^-$ cotransporter, cystic fibrosis transmembrane conductance regulator, anion exchanger 1, and chloride channel 3 in gills of a euryhaline teleost, *Tetraodon nigroviri*dis. *Comp Biochem Physiol A Mol Integr Physiol* 147: 521–528, 2007. doi:10.1016/j.cbpa.2007.01.679.
68. **Tannen RL, Sahai A.** Biochemical pathways and modulators of renal ammoniagenesis. *Miner Electrolyte Metab* 16: 249–258, 1990.
69. **Tresguerres M, Parks SK, Wood CM, Goss GG.** $V\text{-}H^+$-ATPase translocation during blood alkalosis in dogfish gills: interaction with carbonic anhydrase and involvement in the postfeeding alkaline tide. *Am J Physiol Regul Integr Comp Physiol* 292: R2012–R2019, 2007. doi:10.1152/ajpregu.00814.2006.
70. **Ura K, Soyano K, Omoto N, Adachi S, Yamauchi K.** Localization of Na^+, K^+-ATPase in tissues of rabbit and teleosts using an antiserum directed against a partial sequence of the α-subunit. *Zool Sci* 13: 219–227, 1996. doi:10.2108/zsj.13.219.
71. **Verdouw H, Van Echteld CJA, Dekkers EMJ.** Ammonia determination based on indophenol formation with sodium salicylate. *Water Res* 12: 399–402, 1978. doi:10.1016/0043-1354(78)90107-0.
72. **Verlander JW, Miller RT, Frank AE, Royaux IE, Kim Y-H, Weiner ID.** Localization of the ammonium transporter proteins RhBG and RhCG in mouse kidney. *Am J Physiol Renal Physiol* 284: F323–F337, 2003. doi:10.1152/ajprenal.00050.2002.
73. **Walser BL, Yagil Y, Jamison RL.** Urea flux in the ureter. *Am J Physiol Renal Physiol* 255: F244–F249, 1988. doi:10.1152/ajprenal.1988.255.2.F244.
74. **Weiner ID, Verlander JW.** Renal ammonia metabolism and transport. *Compr Physiol* 3: 201–220, 2013. doi:10.1002/cphy.c120010.
75. **Weiner ID, Verlander JW.** Ammonia transport in the kidney by Rhesus glycoproteins. *Am J Physiol Renal Physiol* 306: F1107–F1120, 2014. doi:10.1152/ajprenal.00013.2014.
76. **Weiner ID, Verlander JW.** Ammonia transporters and their role in acid-base balance. *Physiol Rev* 97: 465–494, 2017. doi:10.1152/physrev.00011.2016.
77. **Wheatly MG, Hobe H, Wood CM.** The mechanisms of acid-base and ionoregulation in the freshwater rainbow trout during environmental hyperoxia and subsequent normoxia. II. The role of the kidney. *Respir Physiol* 55: 155–173, 1984. doi:10.1016/0034-5687(84)90020-3.
78. **Wilson JM, Leitão A, Gonçalves AF, Ferreira C, Reis-Santos P, Fonseca AV, Da Silva JM, Antunes JC, Pereira-Wilson C, Coimbra J.** Modulation of branchial ion transport protein expression by salinity in glass eels (*Anguilla anguilla* L.). *Mar Biol* 151: 1633–1645, 2007. doi:10.1007/s00227-006-0579-7.
79. **Wood CM.** Acid-base and ionic exchanges at gills and kidney after exhaustive exercise in the rainbow trout. *J Exp Biol* 136: 461–481, 1988.
80. **Wood CM.** Excretion. In: *Physiological Ecology of the Pacific Salmon*, edited by Groot C, Margolis L, and Clarke WC. Vancouver: UBC Press, 1995, p. 381–438.
81. **Wood CM, Bucking C, Grosell M.** Acid-base responses to feeding and intestinal Cl^- uptake in freshwater- and seawater-acclimated killifish, *Fundulus heteroclitus*, an agastric euryhaline teleost. *J Exp Biol* 213: 2681–2692, 2010. doi:10.1242/jeb.039164.
82. **Wood CM, Caldwell FH.** Renal regulation of acid-base balance in a freshwater fish (1). *J Exp Zool* 205: 301–307, 1978. doi:10.1002/jez.1402050214.
83. **Wood CM, Milligan CL, Walsh PJ.** Renal responses of trout to chronic respiratory and metabolic acidoses and metabolic alkalosis. *Am J Physiol Regul Integr Comp Physiol* 277: R482–R492, 1999. doi:10.1152/ajpregu.1999.277.2.R482.
84. **Wright PA, Wood CM.** A new paradigm for ammonia excretion in aquatic animals: role of Rhesus (Rh) glycoproteins. *J Exp Biol* 212: 2303–2312, 2009. doi:10.1242/jeb.023085.
85. **Wright PA, Wood CM.** Seven things fish know about ammonia and we don't. *Respir Physiol Neurobiol* 184: 231–240, 2012. doi:10.1016/j.resp.2012.07.003.
86. **Wright PA, Wood CM, Wilson JM.** Rh versus pH: the role of Rhesus glycoproteins in renal ammonia excretion during metabolic acidosis in a freshwater teleost fish. *J Exp Biol* 217: 2855–2865, 2014. doi:10.1242/jeb.098640.
87. **Zimmer AM, Nawata CM, Wood CM.** Physiological and molecular analysis of the interactive effects of feeding and high environmental ammonia on branchial ammonia excretion and Na^+ uptake in freshwater rainbow trout. *J Comp Physiol B* 180: 1191–1204, 2010. doi:10.1007/s00360-010-0488-4.
88. **Zimmer AM, Wilson JM, Wright PA, Hiroi J, Wood CM.** Different mechanisms of Na^+ uptake and ammonia excretion by the gill and yolk sac epithelium of early life stage rainbow trout. *J Exp Biol* 220: 775–786, 2017. doi:10.1242/jeb.148429.